Copyright is owned by the Author of the thesis. Permission is given for a copy to be downloaded by an individual for the purpose of research and private study only. The thesis may not be reproduced elsewhere without the permission of the Author.

SURFACE MODIFICATIONS TO INCREASE DAIRY PRODUCTION RUN LENGTH

A THESIS PRESENTED IN PARTIAL FULFILMENT OF THE REQUIREMENTS FOR THE DEGREE OF

MASTER OF CHEMICAL ENGINEERING

at Massey University, [Manawatū], New Zealand.

BY

SIDDHARTH RUNWAL

2013

ABSTRACT

Fouling is the build-up of undesired deposits on surfaces. In the dairy industry, fouling is mainly seen in heat exchangers where dairy fluid is heated or concentrated. It is one of the primary reasons for restricted run length, causing financial losses from downtime, the use of cleaning chemicals and reduced product quality.

Fouling is a complex process and is due to number of factors including the properties of the heat transfer surface. A silica based coating is known to alter the surface properties. This study was carried out to investigate the effect of a silica based coating on fouling by whole milk in a falling film evaporator.

Seven independent trials were conducted. In each trial, a control run was carried out followed by a full cleaning of the equipment and then either another control run or a coating run with pasteurized milk from the same batch. There was a six hour interval between the start of the control run and start of the coating run. Since prolonged milk storage may have some effect on fouling rate, control-control runs were carried out to see the effect of prolonged storage. The results obtained from control-control runs were used in analysing the effect of the coating on fouling rate.

All coating trials showed consistently lower fouling rate as compared with corresponding control trials. The Pearson's correlation coefficient of 0.83 showed a strong effect of coating on the fouling rate. Further, a regression analysis gave a p-value of 0.033, indicating that, at the 96.7% level of confidence, coating reduced the fouling rate. The extent of reduction in fouling rate varied from trial to trial. It was estimated that the coating had the potential to increase the run length by a maximum of 34% under the conditions these experiments were carried out.

ACKNOWLEDGMENTS

I am deeply indebted to my supervisors Prof. A.H.J (Tony) Paterson, Dr. Bipan Bansal and Dr. Owen McCarthy for their immense patience, constant motivation, enthusiasm and never ending spirit. I could not have imagined having better mentors and teachers in my life. Your time and dedication, as my teachers, did not go unnoticed. You have sparked a passion for knowledge that will forever shape who I am.

I would also like to thank all my colleagues at Fonterra Research Centre and my friends whose help, stimulating suggestions and encouragement helped me in all the time of research for and writing of this thesis.

Last but not the least, I would like to thank my family: my parents Dilip Runwal and Shobha Runwal, for supporting me to come this far in my life and my wife Manisha whose patient love enabled me to complete this work.

Thank you all.

Table of Contents

1 Project Overview 1-1
1.1 This Work 1-2

2 Literature review 2-1
2.1 Evaporation 2-1
2.2 Heat transfer in thin film evaporators 2-2
2.2.1 Steam side condensation theory 2-4
2.2.2 Steam properties 2-5
2.2.3 Product side boiling theory 2-6
2.2.4 Milk properties 2-7
2.3 Fouling 2-10
2.3.1 Fouling deposit composition 2-11
2.3.2 Fouling mechanism 2-12
2.3.3 Factors affecting fouling 2-15
2.4 Effect of surface characteristics on fouling 2-18
2.5 Fouling mitigation by surface treatment 2-20
2.6 CONCLUSION 2-20

3 Apparatus and Materials 3-1
3.1 Research Evaporator 3-1
3.1.1 Feed handling system 3-2
3.1.2 Feed Preheat System 3-2
3.1.3 Product transfer 3-3
3.1.4 Calandria design 3-3
3.1.5 Liquid distribution 3-5
3.1.6 Vapour-concentrate separation 3-6
3.1.7 Calandria de-aeration and condensate removal 3-6
3.1.8 Condenser and vacuum system 3-6
3.1.9 Steam supply 3-6
3.1.10 Concentrate handling 3-7
3.2 Materials 3-8
3.2.1 Milk 3-8
3.2.2 Cleaning chemicals 3-8
3.2.3 Coating chemical 3-9

4 Methods 4-1
4.1 Experimental design 4-1
4.1.1 Preliminary Trials 4-1
4.1.2 Parallel design 4-2
4.1.3 Series trials 4-3
4.2 Parallel design experimental setup 4-5
4.3 Experimental procedure 4-7
4.4 Determination of fouling rate 4-9
4.4.1 Calculation of the overall heat transfer coefficient 4-9
4.4.2 Fouling rate and induction time estimation 4-10

5 Preliminary and Parallel Trials: Results and Discussion 5-1
5.1 Preliminary Trials 5-1
5.1.1 Optimization of Evaporation Temperature 5-1

5.1.2 Effect of uncontrolled variables on fouling rate 5-2
5.2 Parallel Design Trials 5-6
5.2.1 Trouble shooting: Superheated steam 5-6
5.2.2 Trouble shooting: Non-condensable gas build up in effect C 5-12
5.2.3 Validation of Parallel Trials 5-16

6 Series trials: Results and Discussion 6-1
..... 6-2
6.1 Induction time and fouling rate of control-control trials 6-3
6.2 Effect of coating on induction time and fouling rate 6-7
6.3 Discussion 6-10
6.4 Estimation of increase in run time due to coating 6-1111

7 Conclusion 7-1

8 References 8-1

9 Appendix 9-1
9.1 Appendix A 9-1

List of Figures

Figure 1-1:Typical milk yield per cow throughout the year (Masse, 2007) 1-1
Figure 2-1: Heat transfer through the evaporator tube 2-3
Figure 2-2: Water boiling curve at atmospheric pressure (Incropera and DeWitt, 1990) 2-6
Figure 2-3: Viscosity of skim milk and whole milk concentrates 2-8
Figure 2-4: Thermal conductivity data for whole milk concentrate 2-9
Figure 2-5: Predicted boiling point elevation for skim milk and whole milk concentrates at 60 ^{o}C 2-10
Figure 2-6: The schematic presentation of the milk fouling process induced by an air bubble at a hot stainless steel surface (Jeurnink *et al.*, 1996a) 2-14
Figure 3-1: Single Effect of Research Evaporator 3-1
Figure 3-2: Feed system of RE 3-2
Figure 3-3: Calandria design for effect C of the RE 3-4
Figure 3-4: Liquid loading system inside the calandria 3-5
Figure 3-5: Steam de-superheating system on the RE 3-7
Figure 4-1: Feed system for parallel configuration 4-6
Figure 4-2: Diagrammatic plots of overall heat transfer coefficient versus time showing the approach to determine fouling rate (m) with an induction time (t_c). 4-11
Figure 4-3:Estimation of induction time and fouling rate in trial RE20 4-12
Figure 5-1: Water trial: Evaporation and steam temperature 5-3
Figure 5-2: Effect of total solids on fouling rate 5-3
Figure 5-3: Effect of evaporation temperature on fouling rate 5-4
Figure 5-4: Effect of temperature driving force on fouling rate 5-4
Figure 5-5: Steam differential temperature profile due to change in differential steam pressure in Effect B 5-7
Figure 5-6: De-superheat system on Research Evaporator 5-8
Figure 5-7: Water supply for de-superheating system 5-9
Figure 5-8: Leak in de-superheat line 5-10
Figure 5-9: Rusted parts of the de-superheating line and the incomplete hollow cone spray nozzle 5-10
Figure 5-10: Hollow cone spray nozzle type on the left and full cone spray nozzle type on the right. 5-11
Figure 5-11: Effect C cyclic variation in steam temperature and steam pressure 5-12
Figure 5-12: Trial RE 11. Parallel milk CONTROL trial on Effect B and Effect C 5-13
Figure 5-13: Bottom of Effect C Calandria 5-14
Figure 5-14: Steam trap on Research Evaporator. 5-15
Figure 5-15: Parallel Trial: Very slight fouling in effect C 5-16
Figure 5-16: Bottom of Effect B (right) and Effect C (left) 5-17
Figure 5-17: Effect B tube 5-17
Figure 5-18: Effect C tube 5-17
Figure 6-1: Induction times in control trials 6-3
Figure 6-2: Fouling rates in control trials 6-3
Figure 6-3: Effect of difference between morning and afternoon runs in the evaporation temperature on the corresponding difference in fouling rate. 6-5
Figure 6-4: Effect of difference between mrning and afternoon runs in temperature driving force on the corresponding difference in fouling rate. 6-6
Figure 6-5: Effect of Coating on Induction times for all series trials 6-7
Figure 6-6: Effect of Coating on Fouling rate 6-8

List of Tables

Table 3-1: CIP regime on RE 3-8
Table 4-1: Summary of parallel and series experimental trials 4-4
Table 4-2: Research Evaporator tube details 4-5
Table 4-3: Operating conditions for Research Evaporator 4-8
Table 5-1: Fouling rate of different evaporation temperatures 5-1
Table 5-2: Correlation coefficient test of uncontrolled variables on the fouling rate 5-5
Table 6-1: Morning run of the series trials 6-2
Table 6-2: Afternoon run of the series trials 6-2
Table 6-3: Results of Pearson's correlation coefficient test on difference between morning and afternoon runs 6-8
Table 6-4: Regression test of difference in fouling rate 6-9

Nomenclature

OPT - On-product time

q - Amount of heat transferred (W)

U - Overall heat transfer coefficient (W/m^2K)

A_i - Heat transfer area (m^2)

ΔT - Temperature driving force (K)

h_c - Convective heat transfer coefficient of condensate film (W/m^2K)

S_s - Thickness of steam-side scale (m)

k_s - Thermal conductivity of steam-side scale (W/m^2K)

S_w - Thickness of foulant layer (m)

k_w - Thermal conductivity of wall (W/m^2K)

S_f - Thickness of foulant layer (m)

k_f - Thermal conductivity of foulant layer (W/m^2K)

h_e - Convective heat transfer of product film (W/m^2K)

N - Number of tubes

d_i - Internal diameter (mm)

L - Length of tube (mm)

RE - Research Evaporator

β-lg - Beta-lactoglobulin

α-la - Alpha-lactalbumin

BSA - Bovine serum albumin

Ig - Immunoglobulin

IEP - Isoelectric point

CIP - Clean in place

NCG - Non-condensate gas

BPE - Boiling point elevation

Chapter 1

1 Project Overview

A daily nuisance in the thermal processing of milk is fouling, an undesirable deposit formed on the heating surfaces. Fouling can cause complete blockages and affects the product quality, thereby restricting the run lengths. A restriction on the run length due to fouling limits a factory's ability to use its heat processing equipment optimally.

In New Zealand, milk production has been on a constant rise from 10 billion litres of milk production in 1998/99 season to 16 billion litres of milk in 2008/09 season thereby creating the need for additional processing capacity each year (Masse, 2007).

Furthermore, milk production on a pasture basis is highly seasonal with a peak in early summer, as shown in Figure 1-1.

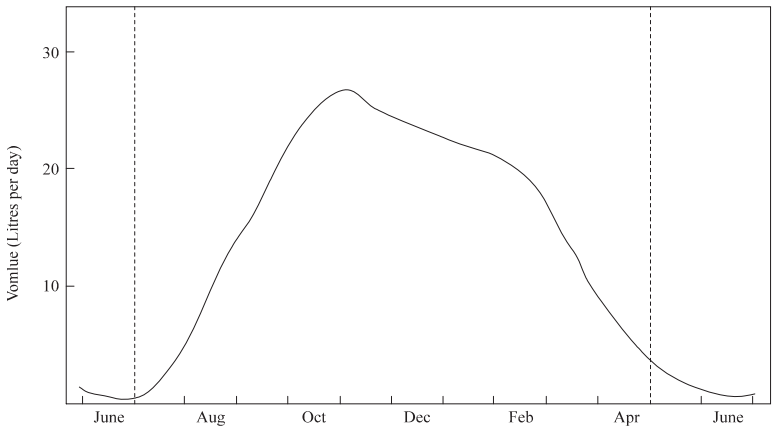

Figure 1-1:Typical milk yield per cow throughout the year (Masse, 2007)

Investment in additional processing capacity to process increased milk production each year is unattractive, as this capacity would only be used during the peak season. The most suitable way to increase the processing capacity, without additional capital investment, is to increase the on-product time (OPT). There has been a drive in Fonterra to reduce fouling since OPT can be increased by longer production runs which are currently limited by fouling.

One of the technologies explored at Fonterra focussed on properties of stainless steel surfaces, a commonly used processing surface in the dairy industry. It is well known that the characteristics of processing surfaces have an impact on fouling (Rosmaninho *et al.*, 2007b; Santos *et al.*, 2004) and by changing these properties, it is possible to delay the onset of fouling. The properties of the processing surfaces can be manipulated favourably by various means, the easiest method being to coat the existing surface using a transient material that has beneficial characteristics which inhibits the build-up of fouling deposit.

A Fonterra technical survey, together with initial lab tests screened a silica based coating which is transient in nature, food grade and non-toxic. Investigations at the laboratory scale and pilot scale showed that this coating was able to successfully reduce the build-up of deposits on convective heat transfer surfaces in plate heat exchangers (Hadfield, 2007).

Falling film evaporators are one of the major heat processing unit operations in the dairy industry that fouls and becomes a bottleneck for production run lengths. Falling film evaporators use a boiling heat transfer mechanism and this project was set up to test the efficacy of coating in falling film evaporators.

1.1 This Work

The overall objective of this project was to investigate the effect of silica based coating on fouling in a falling film evaporator at the pilot scale.

The specific objectives were:

1. To carry out a comprehensive literature review on evaporation, fouling in evaporators and the effect of surface characteristics on fouling.
2. To set up and validate the falling film evaporator at Fonterra Research Centre
3. To establish optimum fouling conditions in the falling film evaporator
4. To investigate the effect of coating on reducing evaporator fouling

Chapter 2

2 Literature review

The main focus of the project was to test the efficacy of coating in reducing evaporator fouling. To design a thorough experimental plan, it was crucial to understand the major aspects: evaporation, fouling and the effect of surface characteristics on fouling.

Thus, the objectives of this section were:

1. To review evaporation in the dairy industry and thermal aspects of falling film evaporation.
2. To review dairy fouling during evaporation including the factors affecting fouling, types of fouling deposit and mechanisms of fouling under nucleate boiling conditions.
3. To review the effect of surface characteristics on fouling and the use of a temporary coating to mitigate fouling.

2.1 Evaporation

The objective of evaporation is to concentrate the solution containing dissolved or suspended solids by boiling off the solvent, generally water. Evaporation is extensively used in processing foods, chemicals, pharmaceuticals, fruit juices, dairy products, and paper and pulp.

In the dairy industry, evaporation is used for concentrating whole milk, skim milk and whey and is used as a preliminary step to drying. Evaporation is less energy intensive than drying and is considered as an important step in making the drying process energy efficient. Evaporation is also used to increase the drier feed viscosity, so that the powder produced has a reasonable particle size and density. Furthermore, evaporation acts as an intermediate step for applying various heat treatments to the milk constituents for obtaining specific functional properties in powders.

To carry out evaporation, heat must be supplied. The products to be evaporated are normally heat sensitive (e.g. whey proteins) and can lose their functionality when subjected to heating for a long time. To reduce this impact, several types of product specific evaporators have been designed. Falling-film evaporators are most suitable for heat-sensitive products due to their short residence time and low evaporation temperatures.

In falling film evaporators, the feed is carefully distributed to the tops of the vertical tubes and then flows down the inner walls. The vapour and the concentrate leave the tubes at the bottom and are separated in a cyclone separator. The tube length can vary from 3 to 18 m. The residence time is less than 1 minute per pass. The thin film of the product reduces the wall temperature required for effective heat transfer. Falling film evaporators work successfully with wall temperatures of 2-3 ^{o}C above the feed boiling temperature. Evaporation in falling film dairy evaporators takes place under vacuum at 65-70 ^{o}C in the first effect to temperatures as low as 40 ^{o}C in the last effect (Mackereth, 1995).

2.2 Heat transfer in thin film evaporators

The basic principle of heat transfer through an evaporator tube is shown in Figure 2-1. Steam condenses on the outside of the tube wall, forming condensate. The heat released is conducted through the evaporator wall to the product film. The heat is released from the product stream by surface evaporation.

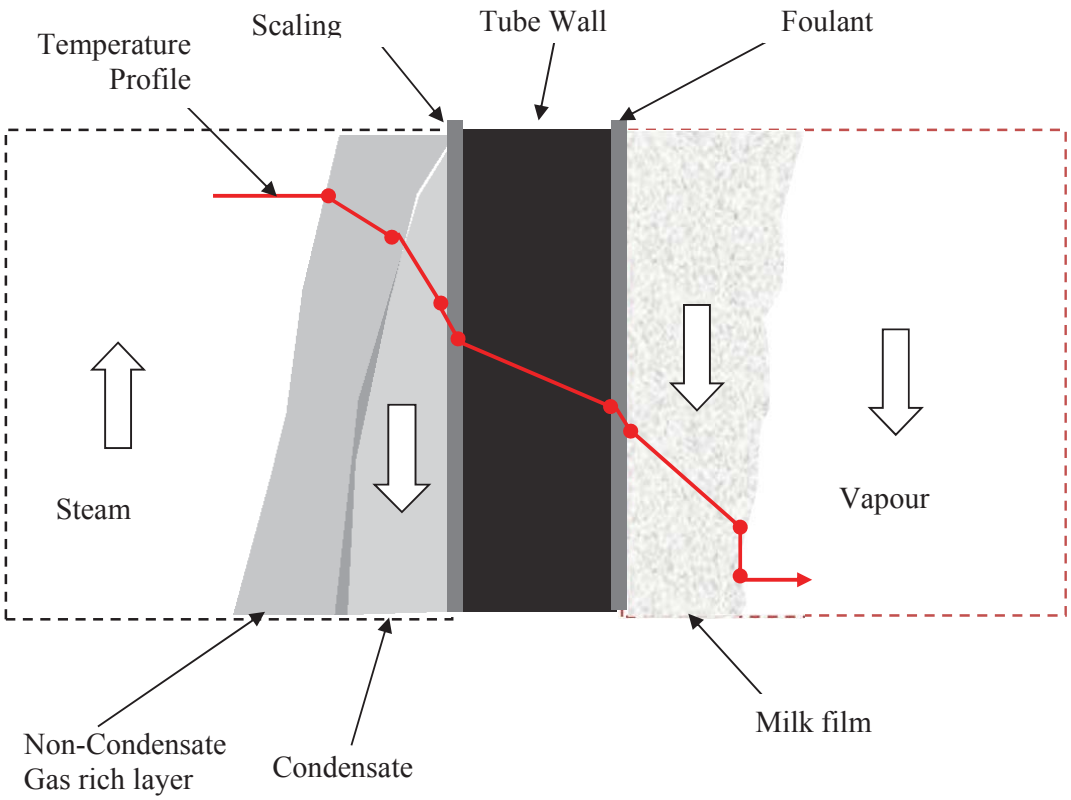

Figure 2-1: Heat transfer through the evaporator tube

The amount of heat transferred is determined by the following equation:

$$\mathbf{q = UA_i\Delta T_U} \qquad \textbf{(Equation 2-1)}$$

Where q is the amount of heat transferred (W), U is the overall heat transfer coefficient (W/m^2K), A_i is the heat transfer area (m^2) and ΔT_U is the difference between the bulk steam saturation temperature and the saturation temperature (K) on the tube side.

The overall heat transfer coefficient, U, takes account of all the properties of the wall, condensate and product streams. The relationship is given in Equation 2-2.

$$\frac{1}{U} = \frac{1}{h} + \frac{S_s}{k_s} + \frac{S_w}{k_w} + \frac{S_f}{k_f} + \frac{1}{h_e} \qquad \textbf{(Equation 2-2)}$$

Where, h_c is the convective heat transfer coefficient of condensate film (W/m^2K), S_s is the thickness of steam-side scale (m), k_s is the thermal conductivity of steam-side scale (W/m^2K), S_w is the thickness of wall (m), k_w is the thermal conductivity of wall (W/m^2K), S_f is the thickness of foulant layer (m), k_f is the thermal conductivity of

foulant layer (W/m^2K) and h_e is the convective heat transfer coefficient of product film (W/m^2K). In this work U has been determined directly by experiment; the calculation procedure is given in Section 4.4.

The area available for heat transfer, A_i, in an evaporator calandria is:

$$\mathbf{A = N\pi d_i L} \qquad \textbf{(Equation 2-3)}$$

Where, N is the number of tubes, d_i is the internal diameter (m) and L is the length of the tube (m).

The steps in the temperature profile between the bulk steam and the bulk product streams are shown in Figure 2.1 as a solid line. The overall temperature driving force, ΔT_U, is defined as the difference between the bulk steam saturation temperature and the saturation temperature of the boiled-off vapour. Each stage of the heat transfer process is governed by a number of factors (equation (2-4).

$$\Delta T_U = \int(\Delta T_{NCG}, \Delta T_c, \Delta T_f, \Delta T_e, \Delta T_w, BPE) \qquad \text{(Equation 2-4)}$$

where subscripts NCG is the non-condensate gases, c is the condensate, f is the foulant material, w is the wall, e is the product film and BPE is the boiling point elevation of the solution being evaporated.

2.2.1 Steam side condensation theory

There are two mechanisms by which vapour will condense on a vertical surface: drop-wise condensation and film condensation. Drop-wise condensation has a higher heat transfer coefficient compared with film condensation.

In drop-wise condensation, the vapour condenses as droplets which grow until they are large enough to run down the surface. The droplets only cover part of the surface at any time and thus there is little resistance to heat transfer. Coatings are usually applied on the surface to make the surface hydrophobic which promotes the drop-wise condensation and thus improves the heat transfer.

Film condensation is the expected mode on clean surfaces. The vapour condenses as a film which thickens as it travels down the tube. At the top of the film the flow is laminar, and then waves start appearing on the surface which introduce a small amount of mixing and also disturb the vapour boundary layer. Eventually, the film will become turbulent.

2.2.2 Steam properties

The presence of superheat and non-condensable gases (NCG) tends to promote film condensation and reduces the overall heat transfer coefficient (Incropera and DeWitt, 1990).

Superheat

The presence of superheat in the steam has a considerable negative effect on the heat transfer rate. This effect increases with the presence of NCG in the steam. The superheated steam must be cooled down to saturation before condensation occurs. The difference between the superheat and saturation temperatures should be subtracted from a measured temperature difference (ΔT_U) to give the true driving force for heat transfer. The presence of superheat in the steam may cause localised hot spots which would lead to rapid product fouling of the tube. Various types of de-superheating systems can be installed, e.g., volume expansion system, direct water spraying, etc. A detailed description of the de-superheating system installed on the Research Evaporator (RE) used in the present work is provided in Section 3.1.

Presence of non-condensable gases

The amount of NCG present in the steam has a major effect on the heat transfer rate. The NCG are drawn to the tube surface along with the condensing steam but remain in the vapour phase. De-aeration ports are usually used to constantly draw NCG out of the shell. The rate of de-aeration is calculated on the basis of the NCG concentration in the incoming steam and the steam flow rate. At low de-aeration rates, the average concentration of NCG at the interface will increase. In an extreme case where the de-aeration port is blocked, for example by condensate flooding, the heat transfer rate slowly drops to approximately half the original rate due to build-up of NCG in the unvented section of the calandria (Mackereth, 1995). A detailed description of the de-aeration port installed on RE and its location is provided in section 3.1.

2.2.3 Product side boiling theory

The nature of boiling on the product side is dependent on the temperature difference between the wall and the product liquid-vapour interface, ΔT_e. The relationship is shown in the Figure 2-2 for water at atmospheric pressure.

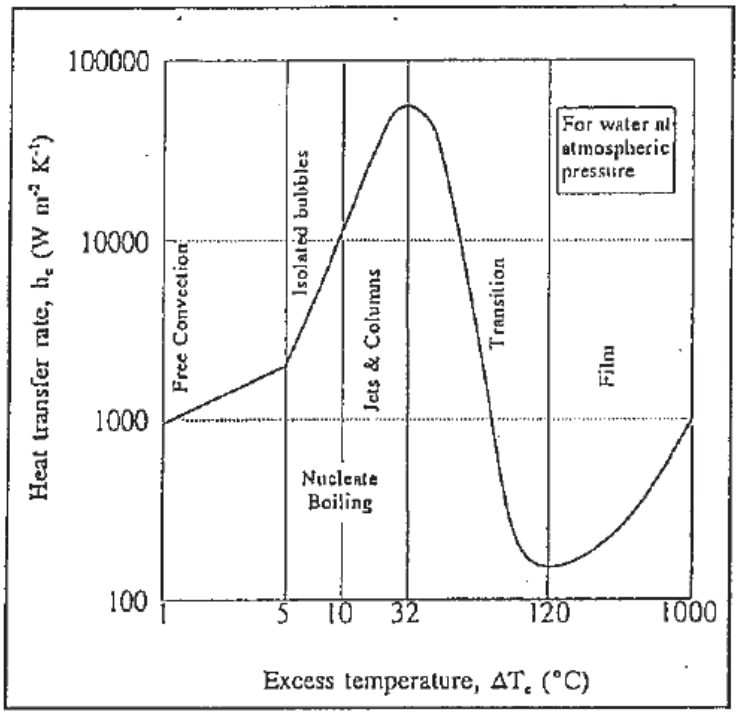

Figure 2-2: Water boiling curve at atmospheric pressure (Incropera and DeWitt, 1990)

With no forced liquid flow at low temperature differences (up to about 5 ^{o}C), free convection boiling occurs. Free convection boiling can be described as surface evaporation where the heat is conducted through the product film and then released by evaporation in the vapour phase. At atmospheric pressure, the nucleate boiling of water will commence at a ΔT_e of 5 ^{o}C. Nucleate boiling involves the formation of bubbles on the wall which grow and travel out to the film-vapour interface. Heat transfer coefficients for nucleate boiling in the absence of fouling are much higher than for free convection boiling. However, as nucleate boiling involves drying out the wall surface, there is a greater potential for fouling than with free convection boiling.

The temperature difference required for nucleate boiling increases when the liquid is flowing over the surface and when the boiling temperature is reduced (Müller-

Steinhagen and Branch, 1997a). When the product film trickles down a tube under gravity the ΔT_e required for nucleate boiling increases to about 7 ^oC (Billet, 1989). Experimental data for the falling film evaporation of water at 50-74 ^oC indicates that the change to nucleate boiling may not occur until $\Delta T_e > 10$ ^oC (Housova, 1970).

For whole milk, the change from free convection boiling to nucleate boiling occurs at a ΔT_e of 0.5 ^oC. The results suggest that foam formation (mainly due to proteins) initiates the nucleate boiling regime at lower ΔT_e in dairy fluids compared to $\Delta T_e > 5$ ^oC for water (Bouman *et al.*, 1993).

2.2.4 Milk properties

Milk properties like viscosity and thermal conductivity change during the evaporation process and affect the heat transfer rate. The heat transfer rate is also affected by the boiling point elevation (BPE) of milk. The changes to milk properties due to evaporation are described in this section.

Viscosity

The viscosity of milk is dependent on milk solids composition, concentration and temperature. Viscosity is known to increase with increasing concentration of milk solids while it decreases with increasing temperature. Various heat-induced changes to milk (e.g. increase in casein micelle size, denaturation of whey proteins and lowering pH) affect the milk viscosity (Anema *et al.*, 2003). The viscosity of milk during the evaporation process varies from 10^{-3} to 0.3 Pa.s (Mackereth, 1995). Figure 2-3 shows the relationship between viscosity and milk solids concentration (Wood, 1982).

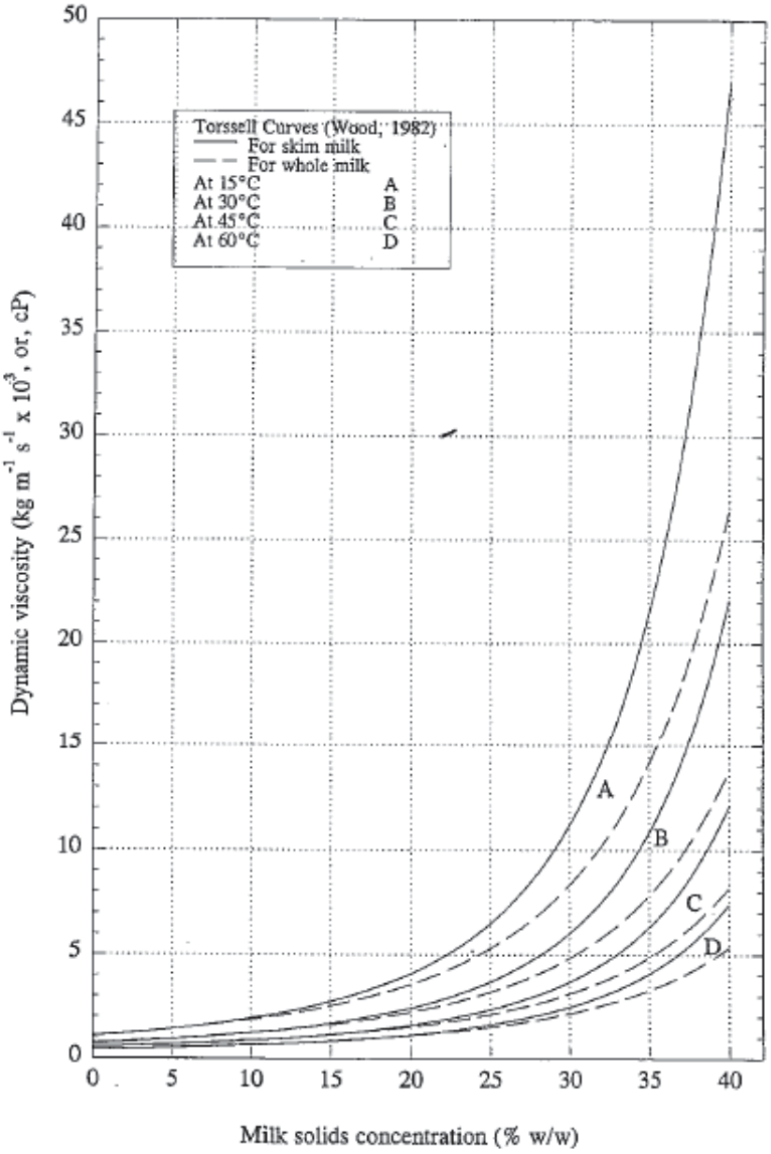

Figure 2-3: Viscosity of skim milk and whole milk concentrates

Thermal Conductivity

The thermal conductivity of whole milk decreases with increasing concentration and increases with increasing temperature. Figure 2-4 shows the relationship between the thermal conductivity of milk and milk concentration at 20 ^{o}C and 80 ^{o}C (Wood, 1982).

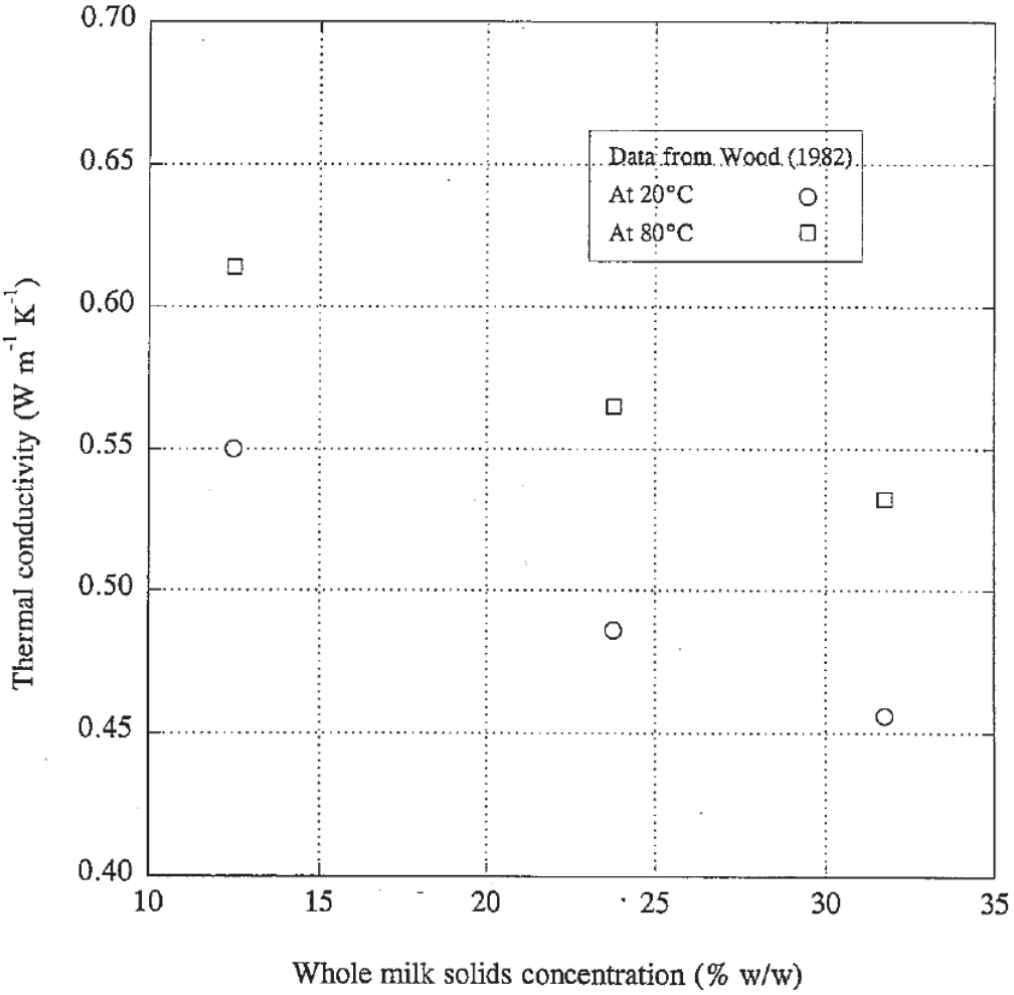

Figure 2-4: Thermal conductivity data for whole milk concentrate

Boiling Point Elevation (BPE)

Aqueous solutions boil at a higher temperature than water because the BPE decreases the effective overall temperature driving force for heat transfer. Hence, high ΔT_U (> 6 -7 ^oC) is applied during final stages of milk concentration (~ 40 – 50 % w/w). BPE data for whole milk is presented below in Figure 2-5 (Wood, 1982).

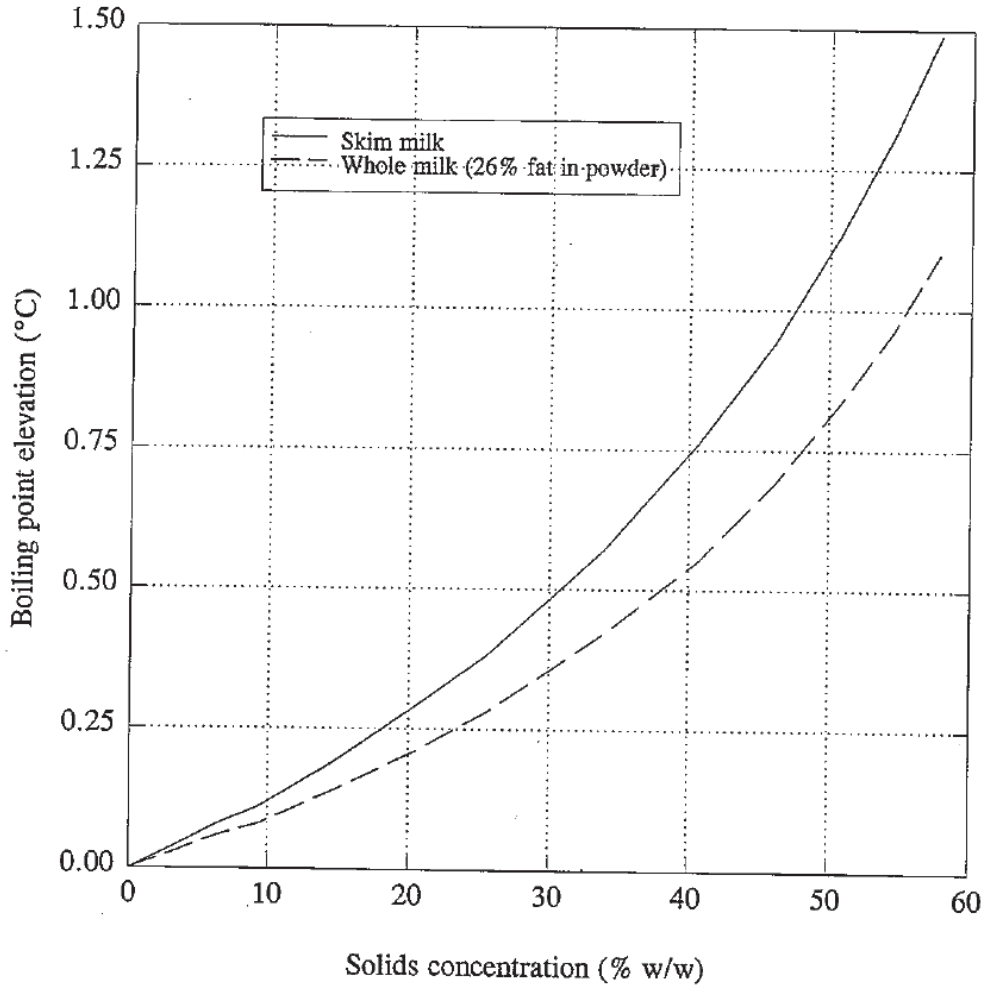

Figure 2-5: Predicted boiling point elevation for skim milk and whole milk concentrates at 60 °C

2.3 Fouling

Heat induced changes in milk constituents, and constituents' interactions among themselves as well as with the processing surface, result in deposit build up on the processing surfaces, described as fouling. Fouling results in reduced heat transfer rates and energy efficiency, poorer yield and a lower product quality due to organic and inorganic contamination in the evaporators.

An understanding of the fouling process will assist in the determination of methods to prevent or delay the undesirable deposit formation on the heat transfer surfaces. Studies that have been carried out to understand fouling can broadly be classified under three headings: fouling deposits, fouling mechanisms and factors affecting fouling.

2.3.1 Fouling deposit composition

The composition of the deposits formed from the milk is largely dependent on the heating temperature of the milk and the heat transfer mechanism.

For convective heat transfer mechanism, two types of deposits have been reported (Burton, 1968).

- The first, called type A, is a voluminous material, which forms at temperatures of around 70 ^{o}C and is a maximum in the range 95 to 110 ^{o}C. The deposit has a high protein content (50 to 70 %) and a lower mineral content (30 to 40 %). At the lower end of the temperature range at which this deposit is formed, most of the protein is (β-lactoglobulin (β-lg), but at the higher end of the range it is predominantly casein (Burton, 1968; Tissier *et al.*, 1985). This deposit is generally soft, white and spongy; however if treated with high temperature for a long time it can become brown and much harder.
- The second type of deposit, called type B, forms at higher temperatures (above 120 ^{o}C) than type A. It is hard and granular, and has a high mineral content (70 to 80 %) and a small amount of protein (10 to 20 %) which is largely casein (Burton, 1965).

For the nucleate boiling heat transfer mechanism the deposit composition reported has been different from type A deposits even though the temperature has been around 70 ^{o}C. A higher fat content has been observed in the evaporator deposits (Jeurnink and Brinkman, 1994). As a part of cleaning studies, a laboratory scale falling film evaporator was run for 20 hours on whole milk before the deposits were analysed. These workers found that the deposits contained 50 % protein, 30 % fat and 20 % minerals (9 % Ca and 12 % PO_4). It was not explicitly mentioned whether the whole milk was recycled or whether fresh milk was supplied continuously during the run.

Another study showed a similar finding after running the evaporator for 25 hours with pasteurised whole milk and skim milk (Mackereth and Grant, 1998). They found that fouling deposits in the evaporator mainly consisted of proteins and fat for the whole milk and proteins for the skim milk. Very low levels of lactose were present in the fouling deposits. Exact percentages of protein and fat were not reported.

A high concentration of fat in the deposit can be attributed to the disruption of fat globules during evaporation. A study (Ye *et al.*, 2005) showed that the size of milk fat globules decreased while the surface protein concentration of the fat globules increased as the milk passed through each effect of the evaporator. The observation indicates that the fat globules were disrupted during DSI preheating and evaporation and the proteins from the milk were adsorbed onto the increased fat globule surface (Ye *et al.*, 2005).

Explicit analysis of the types of whey protein in the deposit was not carried out by either of the above studies. It was not clear whether it was just the whey proteins or a combination of proteins in the deposit composition. Chen (1997) conducted evaporation of cheese whey solution (recycle process) at 70^{o}C in a Centritherm evaporator for 6h and found that bovine serum albumin (BSA) proteins play an important role in fouling in evaporation processes at temperatures lower than 70 ^{o}C. Whereas β-lg and α-lactalbumin (α-la) proteins were seen to be undenatured even after running the evaporator for 6h at 70 ^{o}C. About 72 % of the BSA was reported to be denatured.

2.3.2 Fouling mechanism

A large number of studies have been focussed on the fouling mechanisms using a variety of dairy fluids, processing conditions and analytical techniques.

There is general agreement that at least two separate reactions play an important role during the heating of milk: denaturation and aggregation of whey protein, especially β-lg, and the precipitation of calcium phosphate from solution (Jeurnink *et al.*, 1996b).

In addition to that, a general consideration for a possible fouling mechanism for milk fouling process has been reviewed (de Jong, 1997). The mechanism proposed is distinguished by four independent steps: the formation of particles in the bulk solution

generated by heat; the deposition of these particles onto the heated surface through mass transfer from the bulk liquid to the boundary layer; the adherence of the particles to the surface and a balance between deposition and removal of the particles.

Even though there is an agreement on the type of milk components involved and the general mechanism, there is still an argument about the nature of the initial layer absorbed on the processing surface (Bansal and Chen, 2006; de Jong, 1997).

The results obtained from one study suggest that mineral deposition is crucial in the initial stage of fouling and the minerals are the most likely species to adsorb first (Daufin *et al.*, 1987). This has been supported by another study which describes that the first species formed at the heating surface are minerals. Phosphate ions have been reported as the anion involved in the conditioning of the metal oxide surface prior to the adhesion process (Rosmaninho *et al.*, 2007a; Rosmaninho *et al.*, 2001). Many other researchers support the theory that proteins adsorb first at the surface. Proteins are very surface active and a clean metal surface has a large free surface energy gradient so it would be expected that a protein layer would form very rapidly (Belmar-Beiny and Fryer, 1993).

The majority of the fouling mechanism studies reported have been carried out under convective heat transfer. There is a lack of knowledge of fouling under nucleate boiling heat transfer conditions occurring in the dairy evaporators.

The mechanism of deposit formation under nucleate boiling conditions have been studied for black liquor from the paper and pulp industry (Müller-Steinhagen and Branch, 1997b). It is believed that when bubbles are formed on a heat transfer surface, the solution becomes supersaturated at the vapour-bubble/liquid/solid interface. Micro-layer evaporation at the base of the bubbles causes the local super-saturation of salts in the liquid beneath the bubbles to increase significantly, which results in precipitation and the formation of deposits on the heat transfer surface. A bubble detaching from a nucleation site leaves behind a ring of deposit. If the foulant is highly soluble, it may re-dissolve as the bubble departs; if the solution is supersaturated at the surface conditions, the deposits remain on the heat transfer surface. This process is repeated over a period of time, and therefore, the deposit layer gradually builds up on the surface.

The same mechanism was described for the dissolved air in the milk (Jeurnink *et al.*, 1996a). The enhancement of fouling through air bubble formation on the heated surface was regarded as a distinctive mechanism of milk fouling. Visual observation showed that air bubbles were nuclei for the formation of the deposits. The fouling process induced by the air bubble can be described as follows: when the bubbles are formed, the surface becomes dry and as a result, there is an increase in the temperature difference between the hot stainless steel surface and the bulk of the liquid, resulting in evaporation of water at the vapour-liquid-solid interface. Due to this evaporation, milk is transported from the bulk to the surface where the air bubbles are attached. Here, milk protein accumulates and, because of the local increase in the concentration and the high temperature, the protein may coagulate and deposit on the surface. Eventually the air bubble bursts and part of the accumulated protein is carried away with the liquid. A schematic presentation of this process is shown in the Figure 2-6.

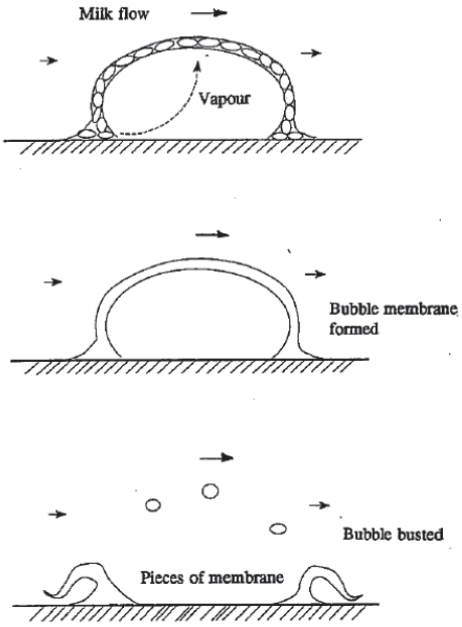

Figure 2-6: The schematic presentation of the milk fouling process induced by an air bubble at a hot stainless steel surface (Jeurnink *et al.*, 1996a)

It is thought that a similar phenomenon may occur in falling film evaporators as a result of nucleate boiling (Jeurnink *et al.*, 1996a).

2.3.3 Factors affecting fouling

Several simultaneous and probably interacting events take place during the heat processing of milk. Combinations of these events are known to affect the fouling process and are reported below.

Milk pH

The reduction in milk pH from the natural fermentation of lactose to lactic acid during storage of milk is reported to affect fouling. The heat stability of casein proteins in milk is highly pH dependent. Milk with a low pH tends to give higher fouling compared to fresh whole milk at normal pH (Burton, 1965).

Milk solids concentration

The deposition rate increased with the rising of the milk concentration (Chen, 1997; Mackereth and Grant, 1998). It was deduced that the increased concentration resulted in higher viscosity and lower turbulence, an increased probability of non-uniform heating. (Chen, 1997).

Calcium concentration

It was reported that either increasing or decreasing the calcium concentration with respect to the normal calcium concentration in milk led to more fouling, due to the effect of calcium on the stability of casein micelles (Jeurnink and Dekruif, 1995). Another study showed that whey fluid depleted of calcium did not produce any fouling and when no precipitable calcium was present, deposit growth was in fact stopped (Daufin *et al.*, 1987). These results are consistent with another study which reported that calcium was essential for the growth of the fouling layer from skim milk and whey (Delsing and Hiddink, 1983).

Whey Protein concentration and structure

Whey proteins are reported by several researchers to be the main constituent present in the deposit composition (Burton, 1965; Visser and Jeurnink, 1997).

Whey proteins can be described as consisting mainly of four compact globular proteins: β-lg, α-la, BSA and several classes of immunoglobulins (Ig). Whey proteins in the

native state are globular proteins having secondary and tertiary structures. The three dimensional globular structure of the individual whey proteins is stabilised by intermolecular disulphide bonds, hydrogen bonds, hydrophobic interactions and ionic bonds. These molecules are highly heat sensitive and have been reported to start to alter their native state upon heating at temperatures as low as 40 ^{o}C (Parris and Baginski, 1991). The alteration causes the protein to partially or completely unfold which exposes its hydrophobic molecular core, together with its reactive disulphide and sulfhydryl (-SH) bonds to an aqueous environment. This state is said to be the state of denaturation. This unstable configuration is stabilised by polymerisation with other denatured molecules in a process known as aggregation. Although denaturation is reversible at low temperatures, as molecules can return to their native state on cooling, aggregation is a totally irreversible process. The rate of aggregation increases significantly above 70 ^{o}C (Galani and Apenten, 1999). Once aggregated, proteins are less soluble and precipitate out.

Even though the exact mechanism of protein adsorption on processing surfaces is unknown, a direct correlation has been established by several researchers between the structure of denatured whey proteins and the rate of fouling (Belmar-Beiny and Fryer, 1993; Jeurnink *et al.*, 1996b).

The role of fat

Fat globules are disrupted during the evaporation process (Ye *et al.*, 2005). Large amounts of water are evaporated during evaporation. Vapour bubbles are formed at the heated surfaces that rapidly travel out to the vapour-liquid interface. Bubbles burst out at the vapour-liquid interface and let the vapour travel out of the liquid film. This causes disruption to the fat globules which results in free fat, fat and casein micelle aggregation or protein and milk fat globule membrane surface protein aggregation. The presence of these complexes are known to promote fouling (Fung *et al.*, 1998).

Heating induced changes in milk

Milk goes through a number of heating steps before drying. At each heating step, milk constituents are degraded and the complexes formed result in different properties in the powder. Many of these heat induced changes are a major cause of fouling.

- Preheating

Milk is preheated prior to evaporation to a temperature of between 75 ^{o}C and 125 ^{o}C and held at the preheat temperature for a period of between 1 s to 3 min. Preheating ensures that the milk temperature is approximately 5 ^{o}C degrees above the first effect evaporation temperature, so that the evaporative heat transfer area is not used for sensible heating. It also ensures that there is some flashing when the milk enters the first effect, which assists in the distribution of the liquids to the tubes. It is reported that preheating denatures whey proteins and forms complexes between β-lg and κ-casein. The soluble form of colloidal calcium phosphate is changed to an insoluble calcium phosphate. It also decreases the milk pH and modifies the casein micelles structure (Singh and Creamer, 1991; Ye *et al.*, 2004).

- Evaporation

Evaporation increases the concentration of solids in the milk prior to homogenization and drying. Whole milk is concentrated from 12 – 13 % w/w to approximately 50 % w/w. Evaporation temperatures range from 70 ^{o}C in the first effect to a minimum of 40 ^{o}C in the last effect. Evaporation causes denaturation of whey proteins. It increases the level of colloidal calcium phosphate. The size of casein micelles are reported to increase during evaporation (Singh and Creamer, 1991). It has also been reported that evaporation causes association of casein micelles and whey proteins with the fat globules (Ye *et al.*, 2004).

Evaporation Temperature

Since chemical reactions are involved in the fouling process it is apparent that temperature is the key factor in the fouling of dairy fluids. Increasing the temperature promotes fouling (Mackereth and Grant, 1998). Fouling deposits were reported to increase with increasing evaporation temperature (Chen and Jebson, 1997).

Induction time

An induction period is the time for the initial layer of fouling to deposit on the surface of the stainless steel. In general, an induction period was suggested to depend upon the condition of the processing surface. The mechanism for the induction period was reported to involve the adsorption of protein and calcium phosphate onto the stainless

steel and induction was mainly considered as a surface and milk constituent interaction (Delsing and Hiddink, 1983).

A study indicated that the induction period was shorter for aged raw fresh whole milk, compared with the initial raw fresh whole milk, when the milk was sterilised at 140 ^{o}C for 2 s (Kastanas *et al.*, 1995). In some cases, there was no induction period for fouling by whole milk (Foster *et al.*, 1989). In tubular geometries an induction period, which is characterised by unchanged conditions of heat transfer and pressure drop, is seen, whereas, in plate heat exchangers, the induction period is less obvious due to the complex exchanger geometry (Fryer *et al.*, 2006). A general observation is that the induction period is reduced and a higher fouling rate is observed when equipment is poorly cleaned.

2.4 Effect of surface characteristics on fouling

Stainless steel is a commonly used processing surface in the dairy industry. Fouling formation is a result of interaction between the processing surface and milk components, hence surface properties influence the type and rate of deposit build up. Surface charge, surface hydrophobicity, chemical heterogeneity and surface roughness are the main properties that have been studied to understand their effect on fouling. It is understood that surface properties play a role only until the first deposit layer is established. This is not surprising as once a surface has become covered with the fouled material it becomes a deposit-deposit interaction rather than deposit-surface interaction (Britten *et al.*, 1988).

Various surface properties have been reported to be affected by one or more naturally occurring oxidation processes, hence studying these properties independently is difficult (Santos *et al.*, 2006). Some general trends in the effects of these properties on fouling have been reported in the literature.

Surface roughness is reported to have no effect on fouling (Yoon and Lund, 1994). Teflon, stainless steel, titanium, polysiloxane and electropolished stainless steel with different surface roughnesses were used to coat a plate heat exchanger surface in their experiment.

Hydrophobic surfaces have been frequently reported to adsorb more protein compared with hydrophilic surfaces (Kang and Lee, 2007; Wahlgren and Arnebrant, 1990). It was found that proteins adsorb on hydrophilic surfaces only if electrostatic interaction is favourable, i.e. if the net charge of the proteins is opposite to that of the surface. However, protein adsorption on hydrophobic surfaces occurred even with the same net charge on the surface and on the protein (Norde and Haynes, 1994). These finding were confirmed when β-lg adsorption on hydrophobic silica, hydrophilic chromium oxide and hydrophilic stainless steel was studied. It was observed that lower amounts of β-lg deposited on the hydrophilic surfaces (Karlsson, 1999). A contradictory result was reported in another study which compared the β-lg adsorption on hydrophobic and hydrophilic silica. In this case, hydrophobic silica was reported to foul less than the hydrophilic silica (Krisdhasima *et al.*, 1992). This contradiction indicates that other properties like chemical heterogeneity may also have a significant influence on the deposit formation.

Stainless steel surfaces used in the industry are rarely chemically homogeneous at the surface. The chromium in stainless steel alloys produces the stainless characteristics through a formation of a chromium oxide rich surface film called a passive layer. The oxide passive layer forms and renews itself in the presence of oxygen, water and/or cleaning chemicals like nitric acid in particular. The composition of the passive layer is chemically heterogeneous over the surface and changes with surface finish. Various properties like surface free energy, hyrophobicity and the isoelectric point (IEP) are influenced by the passive layer and are different for each region (or patch) on the surface, making it chemically heterogeneous. Protein molecules may be adsorbed in different orientations or conformational states depending on the local surface characteristics (Karlsson, 1999). Experiments done on three types of stainless steel alloy prepared with different passivation techniques did not show significant differences in the adsorbed material. It was mentioned that difficulties arose when attempting to predict the nature of alterations in surface charge accompanying the change in Cr/Fe ratio in the oxide film. Consequently, correlating the adsorption behaviour on stainless steel with electrostatic effects was difficult.

2.5 Fouling mitigation by surface treatment

Surface modifications have been reported to affect the initial adsorption rate in the fouling process (Santos *et al.*, 2004). It aims at increasing the induction time of the fouling process and delaying the build-up of deposits.

A fundamental study has demonstrated that a silicate based surface treatment significantly decreased the rate of formation of the initial foulant layer (Parbhu *et al.*, 2006). It was reported that the IEP of the chromium oxide passive layer of industrial grade stainless steel has a value of around pH 9 (Parbhu *et al.*, 2004). The surface becomes negatively charged when the pH of the liquid is higher than the IEP of the material and it becomes positively charged with the pH of the liquid is lower than the IEP of the material. Thus, in the presence of milk (~ pH 6.7), the oxide passive layer has a positive surface charge.

Phosphate anions have been reported in the conditioning of the metal oxide surface prior to the adhesion process (Rosmaninho *et al.*, 2001). β-lg favours adsorption onto calcium phosphate conditioned surfaces. It is also suggested that β-lg and calcium phosphate complex exhibit a strong interaction with the surface allowing protein unfolding with irreversible adsorption. Phosphate ions are negatively charged. The positively charged surface thus favours association with the negatively charged phosphate anions. IEP of the silicate treated chromium oxide surface is reported to be between pH 4-5. So, the silicate treated surface becomes negatively charged in the presence of milk and thus inhibits the association with the phosphate ions and reduces the fouling (Parbhu *et al.*, 2006).

2.6 CONCLUSION

Fouling by whole milk is a complex process and is the result of number of known and unknown factors. Known factors in milk fouling in an falling film evaporator can be broadly classified into four categories: steam properties, milk properties, heat transfer surface properties and process variables such as temperature, pH.

The quality of steam has a considerable impact on the fouling process. The presence of superheat in the steam may cause localised hot spots in a tube which usually lead to rapid fouling by the product.

Milk properties are known to have a greater effect on fouling. Milk of low pH tends to give a higher fouling rate compared with milk of normal pH. Milk with high solids concentrations foul more than milk of normal composition. Also, change in the normal calcium concentration of milk leads to higher fouling rate.

Properties of the heat transfer surface have been shown to influence the fouling process of whole milk. Hydrophobic surfaces have been frequently reported to absorb more protein compared with hydrophilic surfaces. Contradictory reports that suggest no difference in fouling between hydrophobic and hydrophilic surfaces have indicated that the surfaces that are not chemically homogeneous may attract fouling on localised spots with specific free surface energies and hydrophobicities.

Process variables, such as ΔT_e indicates the heat transfer regime. Different heat transfer regimes affect the fouling phenomena in different ways. Nucleate boiling is known to produce air bubbles that move out from the heating surface and burst at the liquid-vapour interface affecting the fat globules in the liquid. This process is known to affect the overall fouling of the liquid.

Milk composition is known to change with time and it is also known that milks with different compositions have different fouling rates.

All these factors were thus reviewed in detail and considered during the design of the experiment.

Chapter 3

3 Apparatus and Materials

3.1 Research Evaporator

A falling film evaporator (herein after referred to as the Research Evaporator, RE) is a vertical shell and tube heat exchanger installed in 1988 in the powder section of the pilot plant at the Fonterra Research Centre. The RE consisted of five single effect evaporator units. A schematic diagram of a single effect is shown in Figure 3-1.

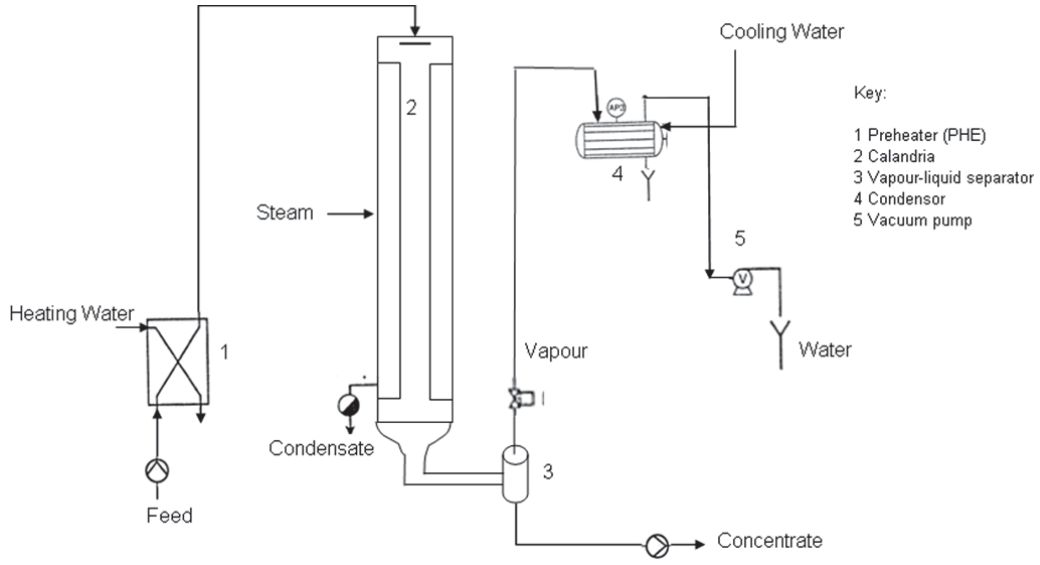

Figure 3-1: Single Effect of Research Evaporator

Each of the five evaporator units (referred to as effect A, effect B, effect C, effect D and effect E) had its own steam supply and independent control of boiling pressure.

A flow plate is installed on the RE for the purpose of changing the configuration of the evaporator effects such that it enables the plant to run as independent effects (only effect A or effect B and so on) or as a combination of effects (effects A, B and C or effects B, C and D or effects C, D and E). The combination of effects is run such that concentrate from one effect feeds the next effect. The RE has a combined maximum evaporative

capacity of 250 - 300 kg h^{-1}. The design of the effects varies from one to another in terms of number, length and diameter of the tubes in each effect. Effect B and effect C were chosen for this work. A detailed description of tubes in each effect and the selection criterion is discussed in Section 4.2.

3.1.1 Feed handling system

Pasteurised whole milk used for all the trials was stored in a 4,000 litre refrigerated silo located on the main floor of the pilot plant. Milk was pumped to the 60 litre tank located in the basement which acted as a feed balance tank to the RE. The feed balance tank along with the milk supply line also had two other supply lines that can feed reticulated soft water coming from the main water line and cleaning-in-place (CIP)/special chemicals pumped from one of the three 500 litre tanks.

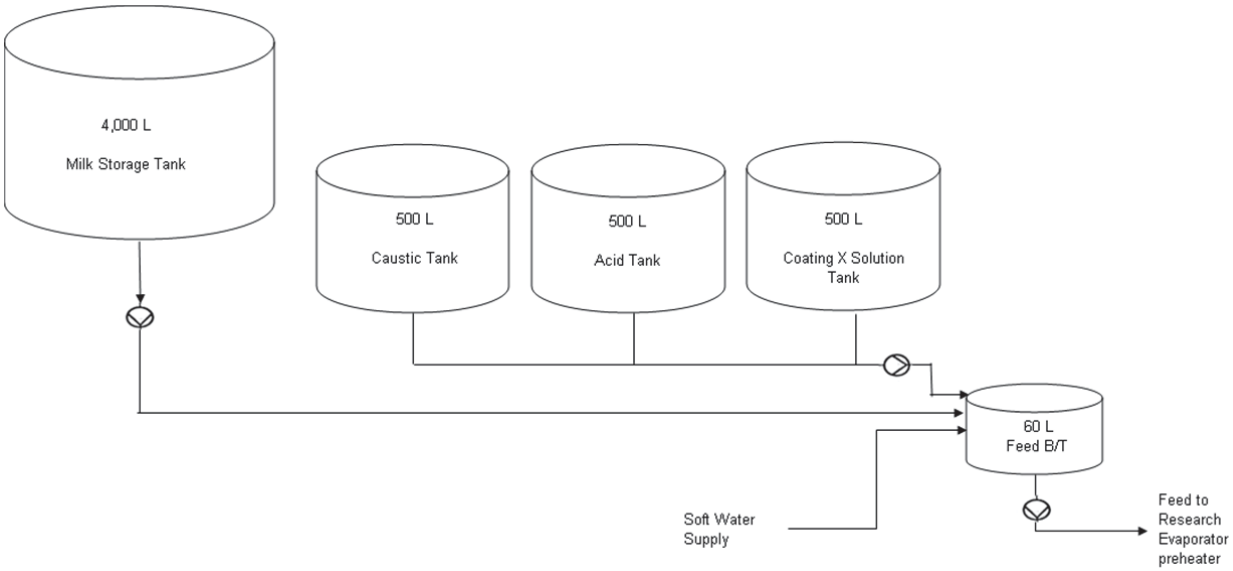

Figure 3-2: Feed system of RE

3.1.2 Feed Preheat System

Feed was preheated to 7 ^{o}C above the evaporation temperature using a plate heat exchanger (Type T4RV, Pasilac Therm A/S, Kolding, Denmark) to ensure sufficient flash occurred in the tube for proper liquid distribution and film formation. The heating water was obtained by mixing cold water and directly injected steam supplied from the pilot plant's main steam supply.

Initially, the feed was preheated only to 5 ^{o}C above the evaporation temperature. But it was realised during the sighter trial that the due to inefficient insulation of the 17 m

long pipe feeding the top of the 15 m calandria, there was a temperature drop of about 3-4 ^{o}C which inhibited flashing in the evaporator tubes. Hence, preheating temperature was raised to 7 ^{o}C to account for the heat loss.

3.1.3 Product transfer

Positive displacement pumps were used on the RE. The pumping of the feed and the concentrate transfer was done using MONO SL range pumps with nitrile rehydrogenerated rubber stators (Model MONO LF502 RO range). These pumps cannot run dry, unlike centrifugal pumps, and hence a feed forward fluid level control with an automatic shutdown system is programmed to avoid damage to the stators.

Stators were damaged on several occasions during the trials and had to be replaced. This caused unsteady feed/concentrate flow and in the worst cases interrupted the trial run. With the fluid level controller being checked and correct, it was thought that high temperature at the feed preheat system might have been the cause. Suppliers were consulted and it was found that the maximum temperature limit for the stators was 110^{o}C, which was well above the operating temperature used in the context of the trials. Owing to the limited time for the trials, this problem was left unresolved. A trial run was continued with an up to 5 % variation in the feed flows. Stators were replaced at the end of the run each time they were damaged. When the variation was more than 5 %, the run was stopped and the stators replaced.

3.1.4 Calandria design

The calandrias of evaporator effect B and effect C were used for this work. A schematic diagram of effect C calandria is shown in Figure 3-3. Effect B is similar to effect C except that effect B has two tubes and effect C has only one tube. The calandrias are 15 m in height and the inside diameter of the tube is 48 mm. It consists of a milk inlet at the top and a liquid distribution plate. A milk film flows on the tube surface and vacuum is pulled from the bottom of the tube. On the shell side, steam enters halfway up the calandria and condensate is removed from the bottom. A sight glass at the bottom of the calandria enables inspecting the condensate level at any time in the calandria. There are two de-aeration ports at the top and bottom of the calandria that are connected to the condenser. Vacuum is pulled on the shell side through these ports. Non-condensate gases (NCG) are continuously removed from the de-aeration ports.

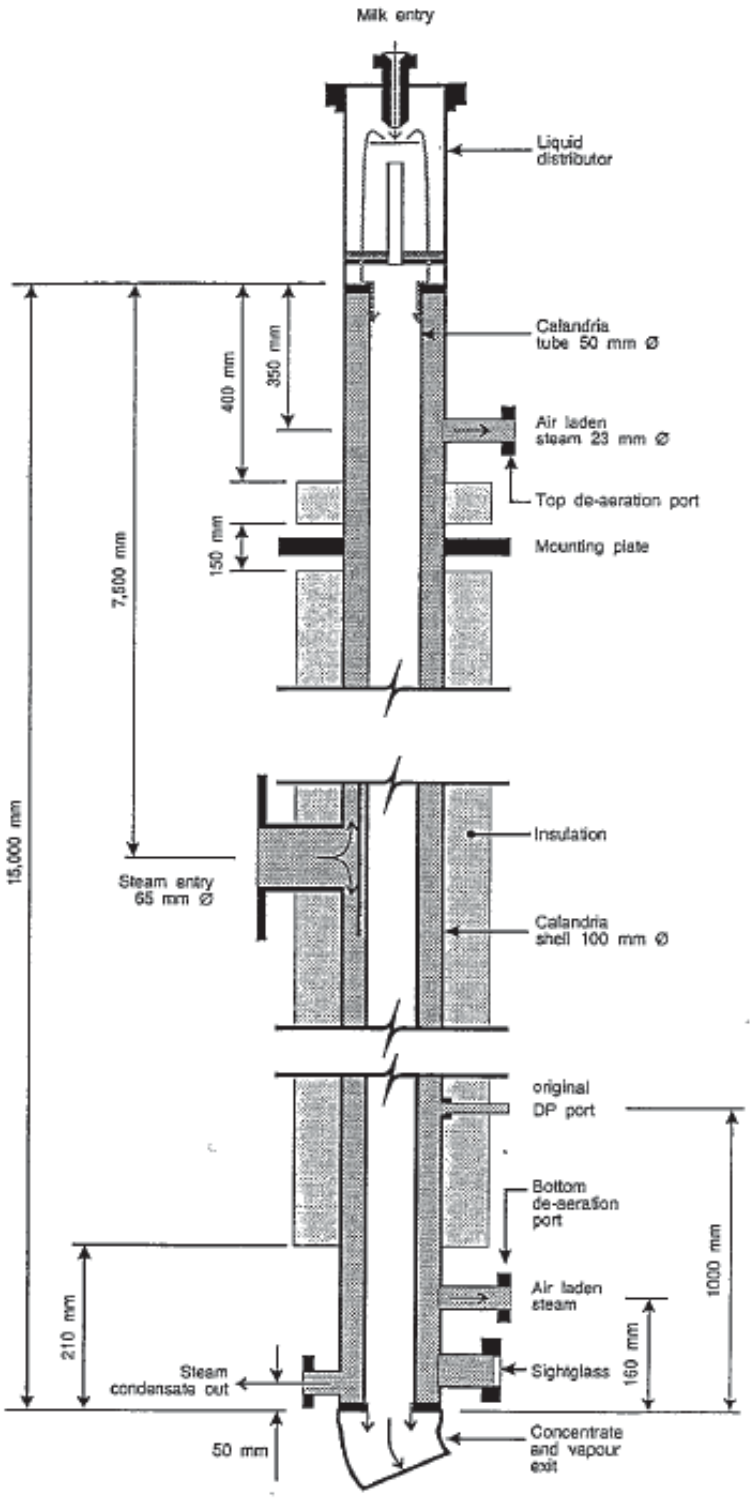

Figure 3-3: Calandria design for effect C of the RE

3.1.5 Liquid distribution

The feed entering the calandria hits a flash plate and flows over onto a distributor plate which has one central vapour riser. Three small holes, on a circle slightly larger than the tube ID, spread the liquid flow around the circumference of the tube. Vapour, flashed off on entry to the calandria, travels through the vapour riser down into the centre of the tube. The liquid stream flows as a film down the tube, while giving off vapour by surface evaporation.

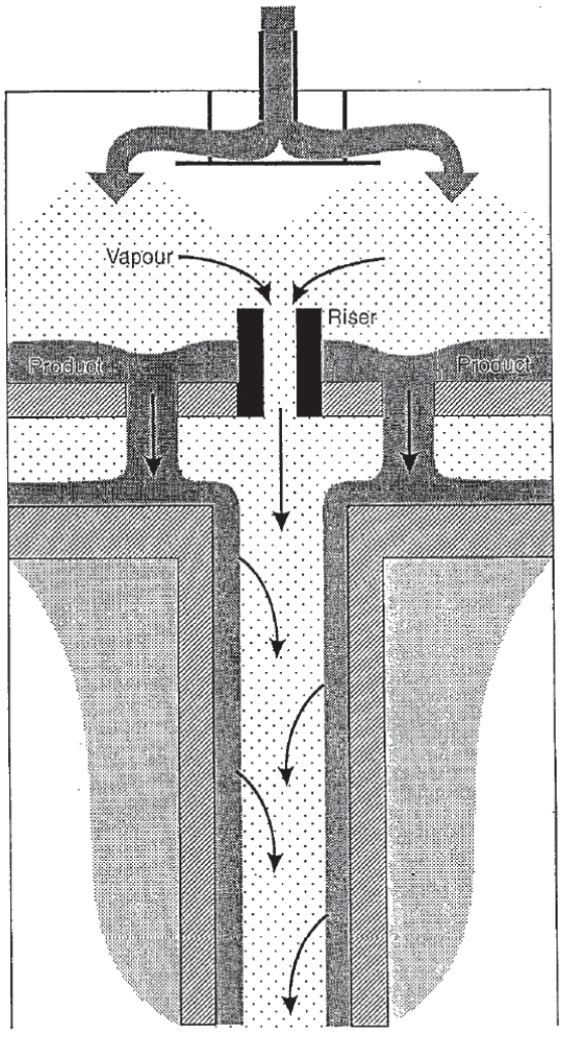

Figure 3-4: Liquid loading system inside the calandria

3.1.6 Vapour-concentrate separation

On leaving the calandria tube, the concentrated liquid and the vapours travel through a short duct via a 90 ^{o}C bend to the vapour liquid separator. A cyclone-type separator is used to separate the liquid from the vapour by centrifugal acceleration. The vapour leaving the separator passes through a control valve to the surface condenser.

3.1.7 Calandria de-aeration and condensate removal

The condensate from each calandria is extracted through a steam trap at the bottom of the calandria and flashed down to the condenser operating pressure. The remaining liquid is gravity fed to the vacuum pump. There is a de-aeration line at both the top and the bottom of each calandria to remove non-condensable gases from the calandria shell. The flow through the de-aeration lines is controlled by an orifice plate. NCG build up was observed a number of times which inhibited heat transfer during the evaporation process. Trouble shooting and the way the NCG build up was observed is discussed in detail in Section 5.2.

3.1.8 Condenser and vacuum system

A surface condenser with a barometric leg is used to condense the boiled-off vapour and extract the condensate. A liquid ring vacuum pump (Model LEM 90, Sihi, Itzehoe, Germany) was used to extract air and other non-condensable gases from the plant.

3.1.9 Steam supply

Steam ran at 9 bar (gauge) in the main header of the pilot plant. It was reduced by two pressure regulators in series to 1.2 bar (gauge) at the calandria. In the case of these trials the steam control valves were set to a fixed manual position. Soft water was sprayed into the steam through a spray nozzle to remove the superheat. Trouble shooting on steam superheat is described in Section 5.2. The location of the de-superheating nozzle is shown in Figure 3-5. A small cyclone separator was employed to remove any excess water added during de-superheating. The excess water was flashed down to the condenser temperature and the remaining liquid was extracted by the vacuum pump. The steam entered the calandria at the midpoint. A deflector plate was installed at the

entrance to distribute the steam evenly and to prevent any solid or liquid material impinging onto the tube(s).

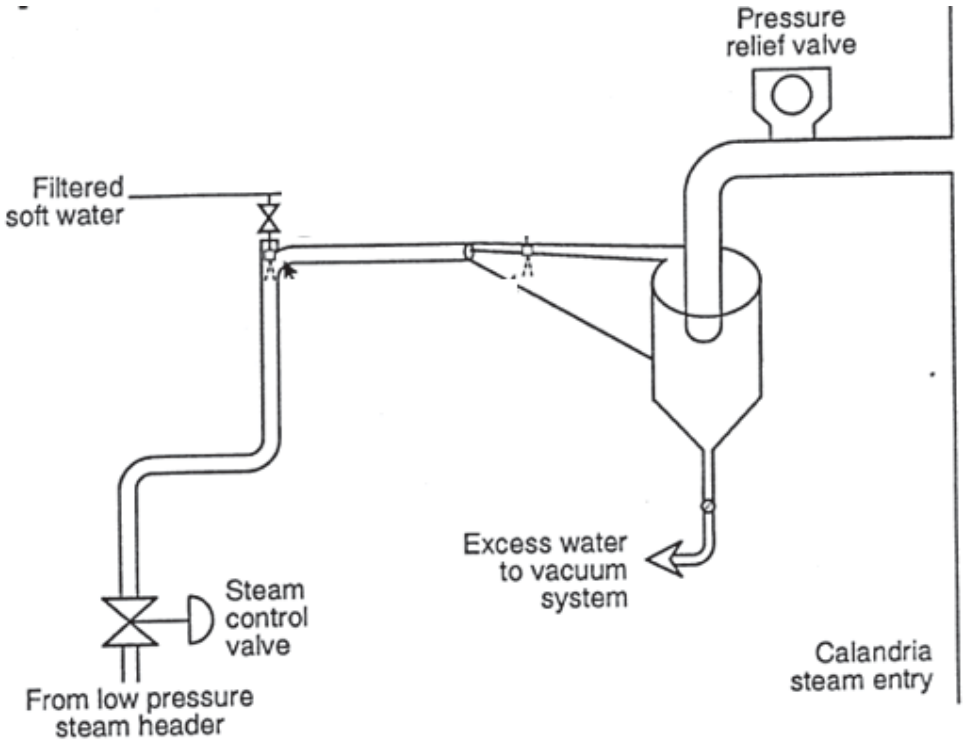

Figure 3-5: Steam de-superheating system on the RE

3.1.10 Concentrate handling

The concentrate leaving the evaporator was fed into a 60 litre concentrate balance tank. The milk concentrate was pumped from this tank to the waste tanks located outside the milk reception area for collection by a local pig farmer. For CIP purposes, a line connected the concentrated tank pump to the milk storage tank on the main level of the pilot plant so that the feed line from the milk storage tank could be cleaned. A drain valve was installed under the concentrate tank to dispose of rinse water and used CIP solutions.

3.2 Materials

3.2.1 Milk

Pasteurised whole milk was used for all trials. Raw whole milk was collected by milk tanker from dairy farms in the Manawatu collection area of the Fonterra Co-operative Group. The milk was collected from several farms and it was not possible to know the exact age of the milk (Duker, 2010). All milk was pasteurised at 72 ^{o}C for 15 s on reception at the Fonterra Research Centre pilot plant milk reception area. Then, the pasteurised milk was kept at 4 ^{o}C before being used for a trial. Trials commenced no later than 6 h after milk pasteurization.

The composition of pasteurised milk was analysed using a Foss Milkoscan S 50 IR spectrometer located in the cheese laboratory of the pilot plant. There was a substantial variation in milk composition from one day to another. Hence, control and coating trials were carried out using the same milk.

3.2.2 Cleaning chemicals

Clean-in-place (CIP) chemicals as described in the RE standard operating procedure were used during the trials. Details of the standard CIP regime done before each trial are shown in Table 3-1..

Step	Concentration (% w/w)	Evaporation Temperature (^{o}C)	Temperature Driving Force (^{o}C)	Time (min)
Water rinse	-	70	5	15
Caustic rinse (NaOH)	1%	70	5	30
Water rinse	-	70	5	15
Acid rinse (Nitrobrite)	1%	70	5	30
Water rinse	-	70	5	15

Table 3-1: CIP regime on RE

1% caustic and acid solutions were prepared in the 500 L tanks connected to the RE's feed balance tank.

3.2.3 Coating chemical

A silica based powder formulation, termed Coating X, was used as a coating material. Coating X was easily dissolved to give an aqueous solution. 200 L of 1% w/v coating X solution was prepared before each coating trial in the 500 L tank connected to the RE's feed balance tank using soft water. The coating procedure is given in Section 4.3.

Chapter 4

4 Methods

4.1 Experimental design

The aim of the experimental design was to investigate the effect of coating in reducing fouling deposits by comparing the fouling obtained in uncoated equipment to the fouling obtained in the coated equipment. The experimental programme was divided into three main sections, described in the following.

4.1.1 Preliminary Trials

There were two main objectives in the preliminary trials.

1. To establish appropriate fouling conditions

   Different fouling rates are obtained at different evaporation temperatures. In commercial evaporators, the evaporation temperature varies from 70^{o}C in the first effect to as low as 40 ^{o}C in the final effect. The fouling rate is known to increase with increasing evaporation temperature.

   For trials in this work, a minimum amount of fouling was desired for comparison between the control and the coating trials. The amount of fouling is dependent on either the evaporation temperature of the trial and/or the length of the trial. Length of trial was limited by the available resources in the pilot plant and hence it was thought necessary to optimize the evaporation temperature to obtain an appropriate fouling rate. Three milk trials were carried out at different evaporation temperatures and the results are discussed in Section 5.1.

2. To investigate the effect of uncontrolled variables on induction time and fouling rate

   a. Evaporation temperature and the temperature driving force were set by manually setting the steam inlet valve and vapour outlet valve positions. Even though the steam valve and the vapour valve were fixed at the same position each time, the evaporation temperature and the temperature driving force inherently varied within a limited range of +/- 1 ^{o}C from

their set points at the start of the trial. It was thus necessary to investigate the effect of this variation on the fouling rate.

b. Day-to-day variation was obtained in milk composition and total solids. The variation in the milk solids was uncontrolled and hence it was essential to investigate its effect on the fouling rate.

Six milk control trials were carried out to investigate the effect of total solids and variation in evaporating temperature and temperature driving force.

4.1.2 Parallel design

It was established from preliminary trials that day-to-day variation in milk solids had a strong effect on the fouling rate. This required that the control and the coating trial be carried out using the same milk for true comparison of fouling rates.

It is reported in the literature that prolonged storage of milk also has an effect on milk composition and might subsequently have an effect on milk fouling. Hence, it was preferred to conduct the control and the coating trials using the same milk at the same time. To this effect a parallel design was implemented. Effect B and effect C were similar effects in the research evaporator. Theoretically, the same heat transfer coefficient would exist in both if they were run at the same processing conditions. The idea was that if the two identical effects showed similar fouling behaviour, then the control and coating runs could be carried out in parallel. The details of the parallel design are given in Section 4.2. Carrying out the control runs and the coating runs at the same time would not only save time but also have the advantage of avoiding any effects due to changes in milk composition caused by milk ageing (prolonged storage of milk) which might have had an effect on milk fouling. An overall objective for these trials was to commission the parallel configuration of the RE and validate that the two effects showed similar fouling behaviour.

Six milk trials (RE11-RE16) were carried out (Table 4-1). While carrying out these trials, a number of technical faults in the RE needed to be corrected. The RE was installed in 1988 and maintenance problems (malfunctioning steam valves, superheated steam, non-condensate gas build up and a vacuum leak) had to be resolved before it

could be used in the parallel design configuration. Parallel trials and troubleshooting work are discussed in Section 5.2.

4.1.3 Series trials

The data from the parallel trials showed that the two effects could not be validated as showing similar fouling behaviours due to an unresolved vacuum leak in effect C. Hence an alternative strategy was used to conduct the trials in series using just effect B. The same milk was used in both the control and coating trials. A full CIP cycle was carried out between the control and coating trials (RE17a,b – RE23a,b).

Since the control and the coating trials were not carried out at the same time in the series trials, changes in the milk composition owing to storage of the milk for the coating trial was accounted for in the experimental design and data analysis. Three control trials (RE18a, RE20a and RE22a) were each carried out during a morning and same three control trials (RE18b, RE20b, RE22b) were each repeated after CIP using the same milk in an afternoon. The differences in the fouling rate in morning and afternoon control trials were considered in the statistical analysis when determining the efficacy of the coating in the four coating trials (RE17a,b; RE19a,b; RE21a,b; RE23a,b). Series trials are listed in Table 4-1 and discussed in Chapter 6.

.

Date	Trial Number	Effect	Sub Number	Condition
Parallel Trials				
12/11/09	RE 11	B	-	Uncoated
		C	-	Uncoated
16/11/09	RE 12	B	-	Uncoated
		C	-	Uncoated
17/11/09	RE 13	B	-	Uncoated
		C	-	Coated
18/11/09	RE 14	B	-	Coated
		C	-	Uncoated
19/11/09	RE 15	B	-	Coated
		C	-	Uncoated
21/01/10	RE 16	B	-	Uncoated
		C	-	Uncoated
Series Trials				
22/01/10	RE 17	B	a	Uncoated
		B	b	Coated
26/01/10	RE 18	B	a	Uncoated
		B	b	Uncoated
28/01/10	RE 19	B	a	Uncoated
		B	b	Coated
29/01/10	RE 20	B	a	Uncoated
		B	b	Uncoated
1/02/10	RE 21	B	a	Uncoated
		B	b	Coated
2/02/10	RE 22	B	a	Uncoated
		B	b	Uncoated
3/02/10	RE 23	B	a	Uncoated
		B	b	Coated

Table 4-1: Summary of parallel and series experimental trials

4.2 Parallel design experimental setup

Two identical effects needed to be set up in parallel so that the control run and the coated run could be carried out at the same time. The RE had five effects. Details are shown in Table 4-2.

Calandria Effects	Number of Tubes	Internal Tube Diameter (mm)	Tube Length (m)
A	4	48	15
B	2	48	15
C	1	48	15
D	1	40	15
E	1 of 3	23 40 48	10

Table 4-2: Research Evaporator tube details

Effect A, effect B and effect C were identical with regard to the internal tube diameter of 48 mm and tube length of 15 m. Effect D and effect E differed from other effects in tube diameter and in tube length, respectively. The most appropriate effects for this work were effect B and effect C. The only difference between the two effects was the number of tubes. This was accounted for by feeding effect B twice as much flow as effect C to obtain the same flow conditions down the tube.

Pasteurised whole milk supplied to both the effects had to be given the same preheat treatment. There was only one preheater available to preheat the feed entering the effects. Hence, the main feed line was split such that the primary feed could be divided into two streams, one for each Effect. Figure 4-1 shows a schematic diagram of the feed system for the parallel configuration.

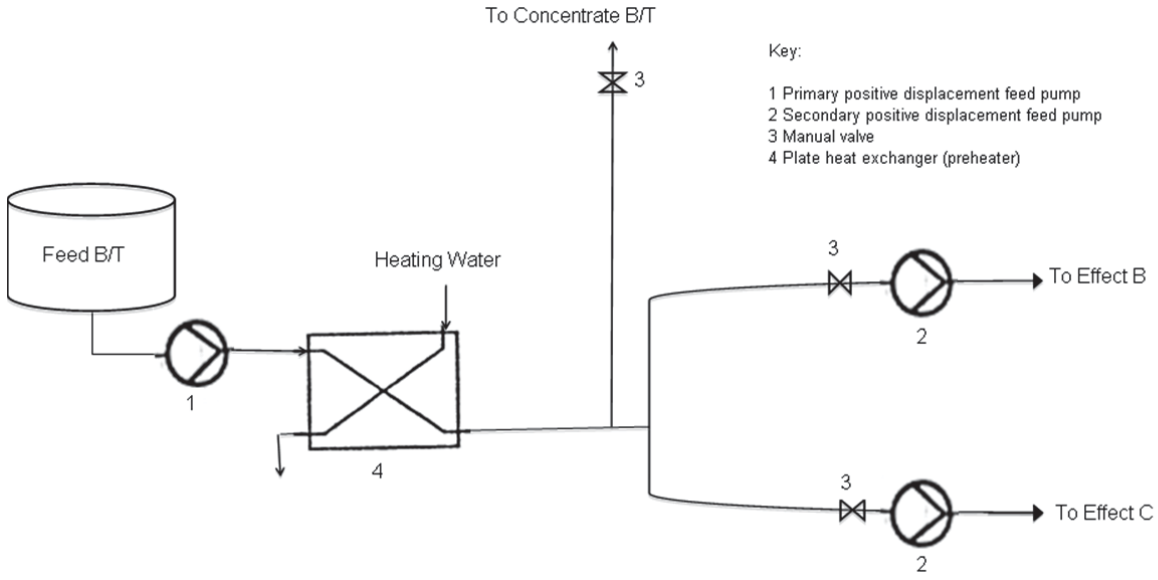

Figure 4-1: Feed system for parallel configuration

It was not recommended to use positive displacement pumps in sequence as it may cause pressure build up in the pipe or might give erroneous flow rates. Hence an additional line was installed between the primary feed pump and secondary feed pumps that acted as pressure relief, going to the concentrate balance tank. Also, to avoid erroneous flow rates, the primary pump was set to a flow rate slightly above (10 L/h) the sum of the flow rates entering the two effects, ensuring enough milk was supplied to the secondary pumps. Continuous excess feed was allowed to go to the concentrate tank. Manual ball valves (key 3 in the Figure 4-1) were installed upstream of the secondary feed pump to vent air at the start to ensure pumps did not run dry due to any air lock in the pipes. This was achieved by keeping the manual valves in open position. The primary pump was started. The line was allowed to flood with the product and only then the manual valves were closed. The secondary pumps were not started before ensuring that the lines were flooded with the product.

4.3 Experimental procedure

The experimental procedure for all milk trials is outlined below.

1. The evaporator was manually assembled in the correct parallel configuration (in the case of parallel trials).
2. Soft water was supplied to the feed balance tank to maintain the level within a desired range.
3. New manual valves were opened to ensure there was no air left in the pipes when the primary feed pump was switched on.
4. The feed pump was switched on according to a procedure which first checked that liquid was available to the pump, and then after starting the pump, checked that the pump was functioning correctly.
5. New ball valve (installed before the pump) on effect B was turned off and the secondary feed pump on effect B was immediately started. The procedure was repeated for effect C (in the case of parallel trials).
6. Concentrate pumps on effect B and effect C were turned on.
7. The vacuum pump was started.
8. When the condenser pressure was less than 10 kPa absolute, effect B and effect C steam valves were opened to 30 % fixed position to warm up the calandria. Steam was also supplied to the plate heat exchanger to preheat the feed to 5 ^{o}C above the evaporation temperature.
9. Effect B and effect C vapour valves at the vapour outlet of the cyclone separator were opened to 30 % fixed position to pull vacuum on the product side.
10. Five minutes later, the steam valves and the vapour valves on both effects were adjusted such that the desired product pressure and differential pressure (between product side and steam side) were obtained. This made sure the product boiling temperature and desired differential temperature was obtained. The valves were operated manually to adjust the pressures and this often required trial and error for fixing the valve position to achieve the desired pressures.

The procedure for the control trial and coating trial differed with an additional coating step included in the coating trial. The procedure is described as follows.

Control trial

11. As the plant reached the steady state, soft water was shut off and the plant was switched to milk.
12. Data was recorded 15 min after the plant remained at steady state.
13. The pressures and temperatures of the plant was monitored during the run and if any abnormal event occurred, it was accounted for while analysing the data.

Coating trial

11. Coating solution was supplied to the feed balance tank. The coating solution was freshly prepared at the start of each trial.
12. Fresh coating solution was fed to the RE for 20 min at evaporation temperature of 70^{o}C and ΔT_U of 3^{o}C. The concentrate at the end of the plant was drained.
13. A 15 min soft water flush step followed the coating step before the plant was switched on to milk.
14. Milk was supplied to the feed balance tank and soft water was shut off.
15. Data in the form of product pressure, product temperature, differential pressure and differential temperature was recorded 15 min after the plant had gained steady state.
16. The pressures and temperatures of the plant were monitored during the run and if any abnormal event occurred, it was accounted for while analysing the data.

The following operating conditions were used for all the control and coating trials unless otherwise specified.

Parameters	**Effect B / Effect C**	
Product flow rate	Effect B (2 tubes)	200 L/h
	Effect C (1 tube)	100 L/h
Milk silo temperature	4 ^{o}C	
Preheat Temperature	80 ^{o}C	
Product temperature (ProdTemp) at t = 0 h	78 ^{o}C	
Temperature difference (TempDiff) at t = 0 h (steam temperature – product temperature)	5 ^{o}C	

Table 4-3: Operating conditions for Research Evaporator

4.4 Determination of fouling rate

4.4.1 Calculation of the overall heat transfer coefficient

Reduction in the overall heat transfer coefficient (U) over time due to fouling deposition is one of the measures used to estimate fouling in evaporators. Rearranging Equation 2.1 gives:

$$\mathbf{U} = \frac{q}{A_i \Delta T_U} \qquad \textbf{(Equation 4-1)}$$

The overall heat transfer coefficient (U) can indirectly be obtained by measuring the temperature difference (ΔT_U, steam temperature – product temperature) across the heating surface, provided other operating parameters (the flow rates of the product and heating medium, the product inlet temperature and heating medium inlet temperature) are kept constant.

In commercial evaporators, as the run progresses, the flow rate of the heating medium is altered to counter the effect of the change in the temperature differential (ΔT_U) due to build-up of deposits on the heat transfer surface. Thus, the overall heat transfer rate is kept constant to achieve consistent total solids in the concentrate.

In the RE, to determine the reduction in heat transfer coefficient, the steam and the vapour control valves were set to fixed positions to give constant mass flow rates and the reduction in the heat transfer coefficient was calculated by measuring the change in temperature difference (ΔT_U).

30 s data were obtained from the data logging system under steady state conditions and all the parameters in Equation 4.1 were calculated using the following equations.

Amount of heat transferred, q

$$\mathbf{q} = \mathbf{q}_{\textbf{Total Evaporation}} - \mathbf{q}_{\textbf{Flash Evaporation}} \qquad \textbf{(Equation 4-2)}$$

Where,

$$\mathbf{q_{Total\ Evaporation}} = (\mathbf{m_{feed}} - \mathbf{m_{concentrate}})\lambda_{\mathbf{AP}}$$

$$q_{Flash\ Evaporation} = m_{feed}\left(h_{f_{T_{feed}}} - h_{f_{T_{product}}}\right)$$

where m is the mass flow rate (kg/h), λ is the latent heat of vaporisation of water (kJ/kg), the subscript AP is the absolute pressure of the product (kPa), h_f is the enthalpy of milk at the specific temperature and total solids (kJ/kg) and T is the temperature (^oC). The calculation to estimate the enthalpy of milk has been given in Appendix A. For calculating flash evaporation, the mass flow rate (kg/h) before and after flash was assumed to be the same as the amount of flash was samll and could be ignored.

Temperature difference, ΔT_U.

$$\mathbf{\Delta T_U = T_{Steam} - T_{Product}} \qquad \textbf{(Equation 4-3)}$$

where T is the temperature (^oC).

Area, A_i

$$\mathbf{A_i = \pi N d_{ID} L} \qquad \textbf{(Equation 4-4)}$$

Where, N is the number of tubes in the calandria, d_{ID} is the internal diameter (m) and L is the length of the tube (m).

4.4.2 Fouling rate and induction time estimation

A linear regression procedure was used to calculate the fouling rate and the induction time from the overall heat transfer coefficient data. In the mathematical model, two linear regression lines were fitted using the least squares method: the first a horizontal line (zero change in ΔT_U), the second line of constant negative slope (indicating the fouling rate). The approach is shown diagrammatically in Figure 4-2.

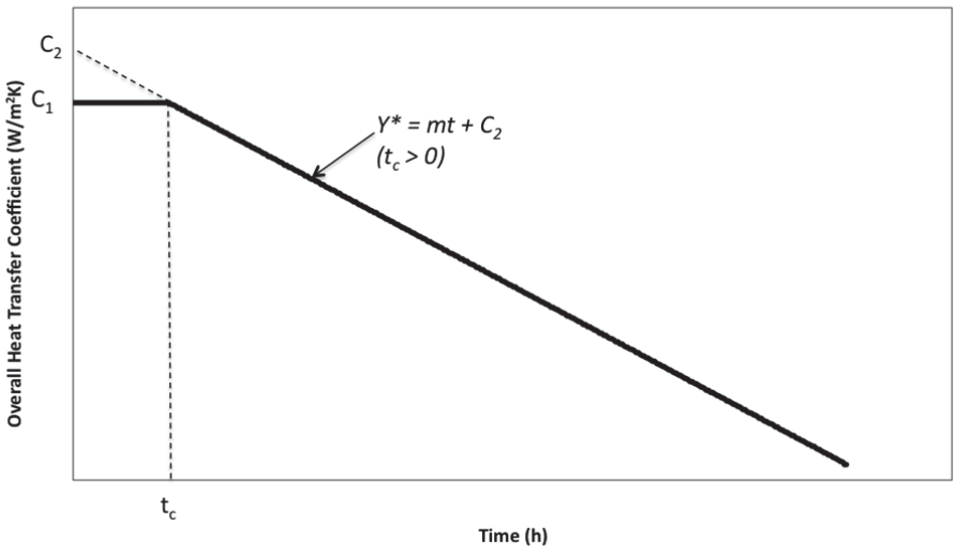

Figure 4-2: Diagrammatic plots of overall heat transfer coefficient versus time showing the approach to determine fouling rate (m) with an induction time (t_c).

The solid line in Figure 4-2 shows the curves as fitted by the least squares analyses. C_1, C_2 and m were the parameters adjusted to minimise the residual sum of squares.

$$y^* = mt + C_2 \quad \text{..... (For } t > t_c\text{)}$$

$$y^* = C_1 \quad \text{.....(For } t < t_c\text{)}$$

Where,

y* = predicted heat transfer coefficient

$$t_c = \frac{(C_1 - C_2)}{m}$$

m = fouling rate

The solver function in Microsoft Excel was used to find the values of C_1, C_2 and m that minimised (absolute) ABS (y – y*), where y = measured heat transfer coefficient.

This approach gave a standard method of estimation of the fouling rate and the induction time from the raw heat transfer coefficient data. Figure 4-3 below shows the experimental data from trial RE20 fitted with this model.

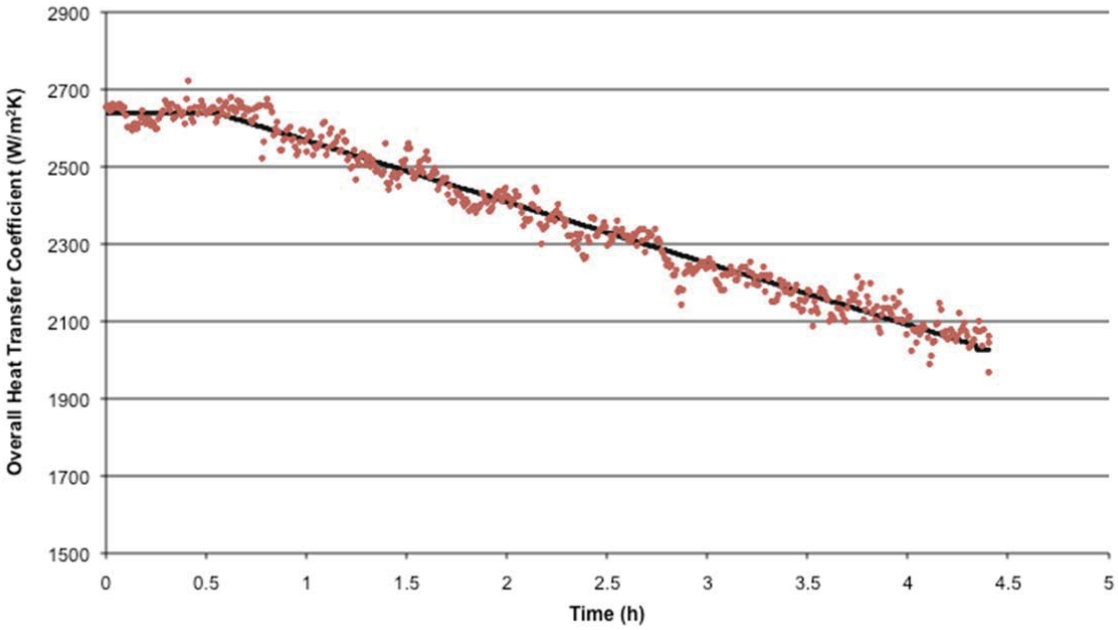

Figure 4-3:Estimation of induction time and fouling rate in trial RE20

The best fit of the data gave an induction period of 0.54 h and fouling rate of 158.8 $W.m^{-2}.K^{-1}.h^{-1}$.

Chapter 5

5 Preliminary and Parallel Trials: Results and Discussion

5.1 Preliminary Trials

Preliminary trials were carried out to establish the right fouling conditions in the RE and to determine the effect of uncontrolled variables on the fouling rate.

5.1.1 Optimization of Evaporation Temperature

A minimum amount of drop in overall heat transfer coefficient (at least 500 W/m^2K) was desired to ensure that the comparison of the fouling rate of control trial versus the fouling rate of coating trial was not ambiguous.

The extent fouling could be altered either by carrying out trials for longer or by increasing the evaporation temperature. Two runs needed to be carried out in series trials using the same milk. The prolonged storage of milk can have detrimental effects on milk composition and hence there was a limitation on increasing the trial run length. The aim was to carry out both runs of a series trial on the same day. The focus, therefore, was to alter the evaporation temperature to achieve both runs of the series trials on the same day with a minimum amount of the desired drop in overall heat transfer coefficient. Three milk trials were conducted on effect B at different evaporation temperatures. Table 5-1 shows the fouling rates in these trials.

Trial numbers	Evaporation Temperature (^oC)	Fouling Rate ($W.m^{-2}K^{-1}\ h^{-1}$)
RE05	71	21
RE07	75	24
RE11	79	113

Table 5-1: Fouling rate of different evaporation temperatures

Different milk batches were used for the different trials. Fouling rate not only depends on the evaporation temperature but also on the total solids of the milk. But since the

total solids of the milk was an uncontrolled variable, only evaporation temperature was considered for this analysis.

A fouling rate of less than 50 $W.m^{-2}K^{-1}$ h^{-1} would require at least a 10 hour trial length to achieve total drop of 500 $W.m^{-2}K^{-1}$. A trial length of 10 hours was considered to be impractical at least in the series trials where milk would have been needed to be stored for 24 hours for the subsequent second run of the series trial.

An evaporation temperature of 79 ^{o}C gave a fouling rate above 100 $W.m^{-2}K^{-1}$ h^{-1} which required 5 hours to achieve a drop of in the overall heat transfer coefficient 500 $W.m^{-2}K^{-1}$ and this was considered reasonable. Hence, 79 ^{o}C was decided to be the evaporation temperature to achieve the required fouling rate.

5.1.2 Effect of uncontrolled variables on fouling rate

Variation in milk composition and total solids, variation in the evaporation temperature and variation in the temperature driving force at t = 0, were identified as the uncontrolled variables in the RE milk trials which might have had an effect on the fouling rate.

The evaporation temperature and the temperature driving force were fixed at the start of the run to 79 ^{o}C and 5 ^{o}C respectively by fixing the steam valve and the vapour valve position to a fixed value. Though the valve positions were fixed, there was an inherent variation of +/- 1^{o}C in the both temperatures that could not be controlled. It was thus necessary to account for this initial variation and determine its effect on the fouling rate.

As the run progressed, the gradual change in the evaporation temperature and temperature driving force was assumed to be the function of fouling. This was confirmed by carrying out a water trial. Figure 5-1 shows a water trial where the evaporation and the steam temperature remained constant over the length of the run. Hence, only the starting points were considered to see the effect of variation in both the evaporator temperature and temperature difference on fouling rate.

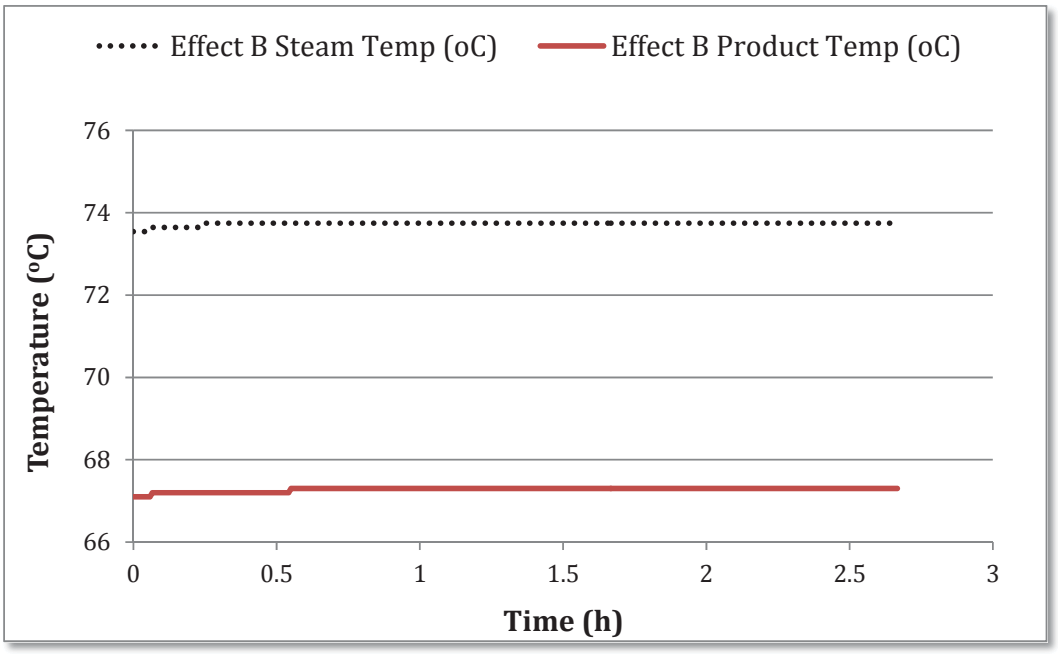

Figure 5-1: Water trial: Evaporation and steam temperature

Seven milk control trials (RE17a-23a) were used to investigate the effects of these uncontrolled variables. Figure 5-2, Figure 5-3 and Figure 5-4 show the scatter plot of the variation in total solids, evaporation temperature and temperature driving force on the fouling rate.

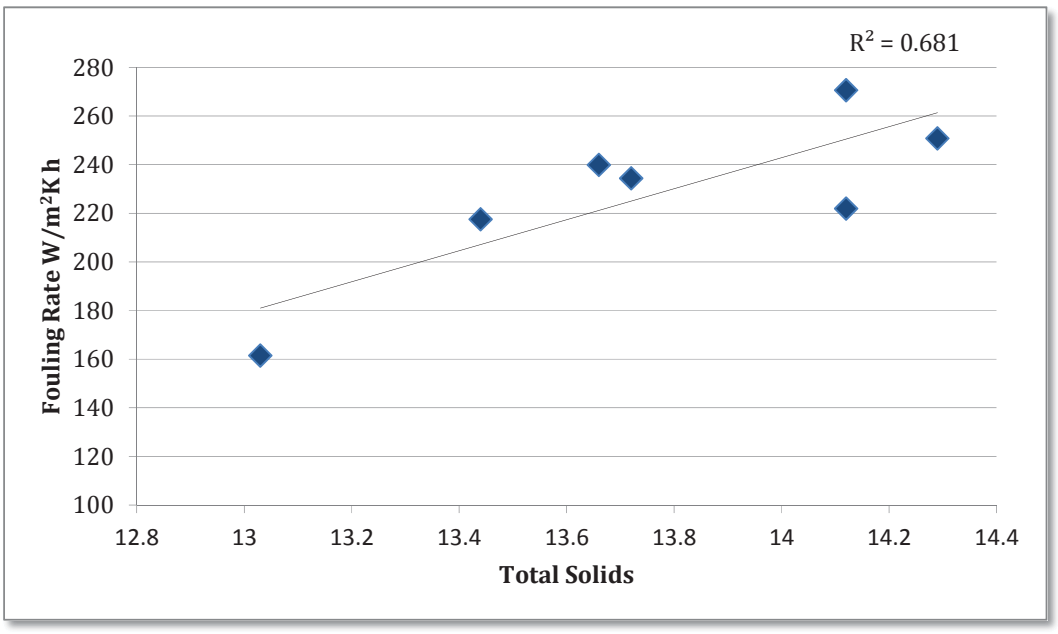

Figure 5-2: Effect of total solids on fouling rate

RE17a to RE23a were carried from 22/01/10 to 03/02/10. Different milk was used for each trial. Seven data points in Figure 5-2 show the milk total solids for each trial.

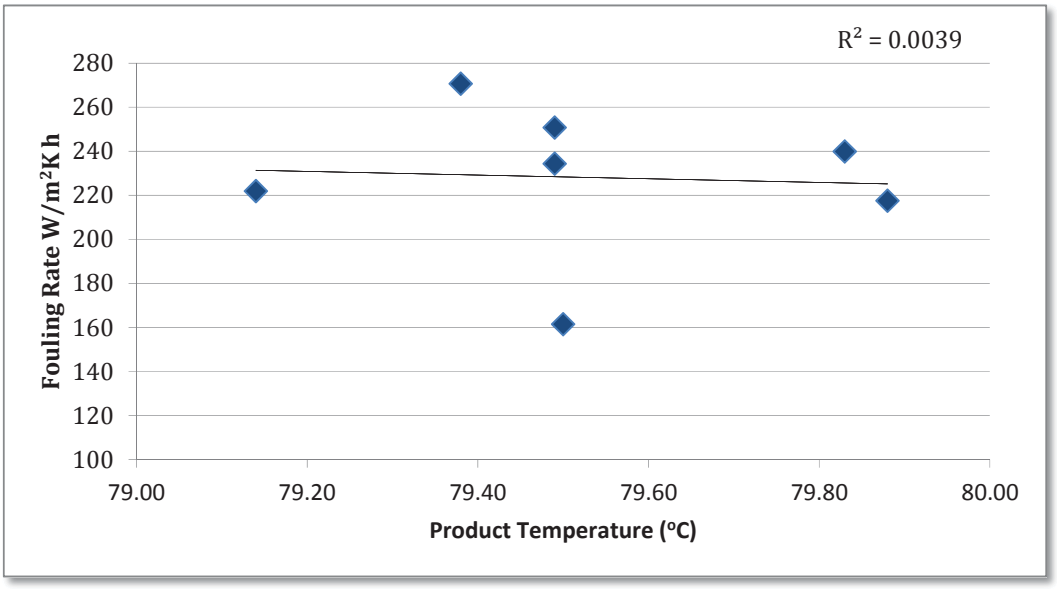

Figure 5-3: Effect of evaporation temperature on fouling rate

The initial evaporation temperature of each individual trial was set to 79 °C. Figure 5-3 shows the inherent variation of +/- 0.4 °C of the evaporation temperature within each trial.

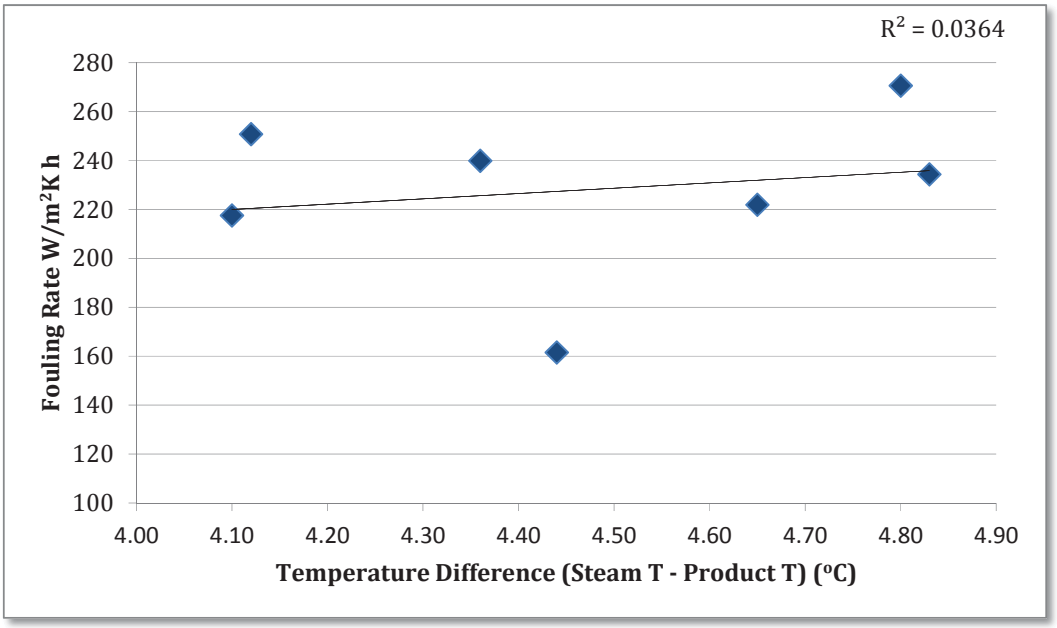

Figure 5-4: Effect of temperature driving force on fouling rate

The initial temperature driving force was set to 4.5 ^{o}C to ensure the nucleate boiling heat transfer mechanism occurred in the evaporation tubes. Above graph shows the +/- 0.4 ^{o}C variation with each trial.

A Pearson's correlation coefficient test was carried out for each of the uncontrolled variables using the seven data points. Table 5-2 show the results.

	Total Solids	*Evaporating Temperature*	*Temperature Driving Force*	*Fouling Rate*
Total Solids	1			
Evaporating Temperature	-0.49	1		
Temperature Driving Force	0.17	-0.61	1	
Fouling Rate	0.83	-0.06	0.19	1

Table 5-2: Correlation coefficient test of uncontrolled variables on the fouling rate

The Pearson correlation is +1 in the case of a perfect positive (increasing) linear relationship, −1 in the case of a perfect decreasing (negative) linear relationship, and has some value between −1 and 1 in all other cases, indicating the degree of linear dependence between the variables. As it approaches zero there is less of a relationship (closer to uncorrelated). The closer the coefficient is to either −1 or 1, the stronger the correlation between the variables.

The fourth row in the table shows individual correlation coefficients for the relationships between total solids, evaporation temperature and the temperature driving force on the one hand and fouling rate on the other. Total solids were strongly correlated with fouling rate. Fouling rate was only weakly dependent on evaporation temperature and temperature driving force.

Since there was a strong dependence of fouling rate on milk total solids, it became clear that the same milk should be used when comparing the fouling rate of the control (uncoated) trial with the fouling rate of the coated trial.

5.2 Parallel Design Trials

Effect B and effect C are similar to each other and theoretically comparable heat transfer coefficients should be expected when running both effects at the same processing conditions. The main objective of this work was to validate effect B and effect C in parallel to enable a system for conducting coating trials.

In the first few sighter trials that were carried out, it was realised that the process variables like the steam temperature, steam pressure and the product pressure were not consistent with their set points during the length of a trial run on effect B and effect C. In order to validate effect B and effect C in parallel, it was important to resolve these issues.

Specific experiments with water were thus carried out to understand the cause of the variation and subsequently to resolve the problems. Data from the initial water trials are shown and discussed below. Water trials were carried out in a fashion similar to that described in Section 4.3 except that water was used as the test fluid instead of milk.

5.2.1 Trouble shooting: Superheated steam

In the initial sighter milk trials, it was realised that the steam temperature did not correlate with the saturated steam pressure. To confirm this in the water trial, step changes in the steam pressure were made to see their effect on the steam temperature. The steam control valve was manually opened to step increase the steam pressure and the steam temperature was monitored. Theoretically it was expected that the steam temperature would increase by the equivalent amount to the steam pressure and remain stable at the saturated steam conditions pertaining.

Figure 5-5 shows differential pressure on the primary Y-axis and differential temperature on the secondary Y-axis.

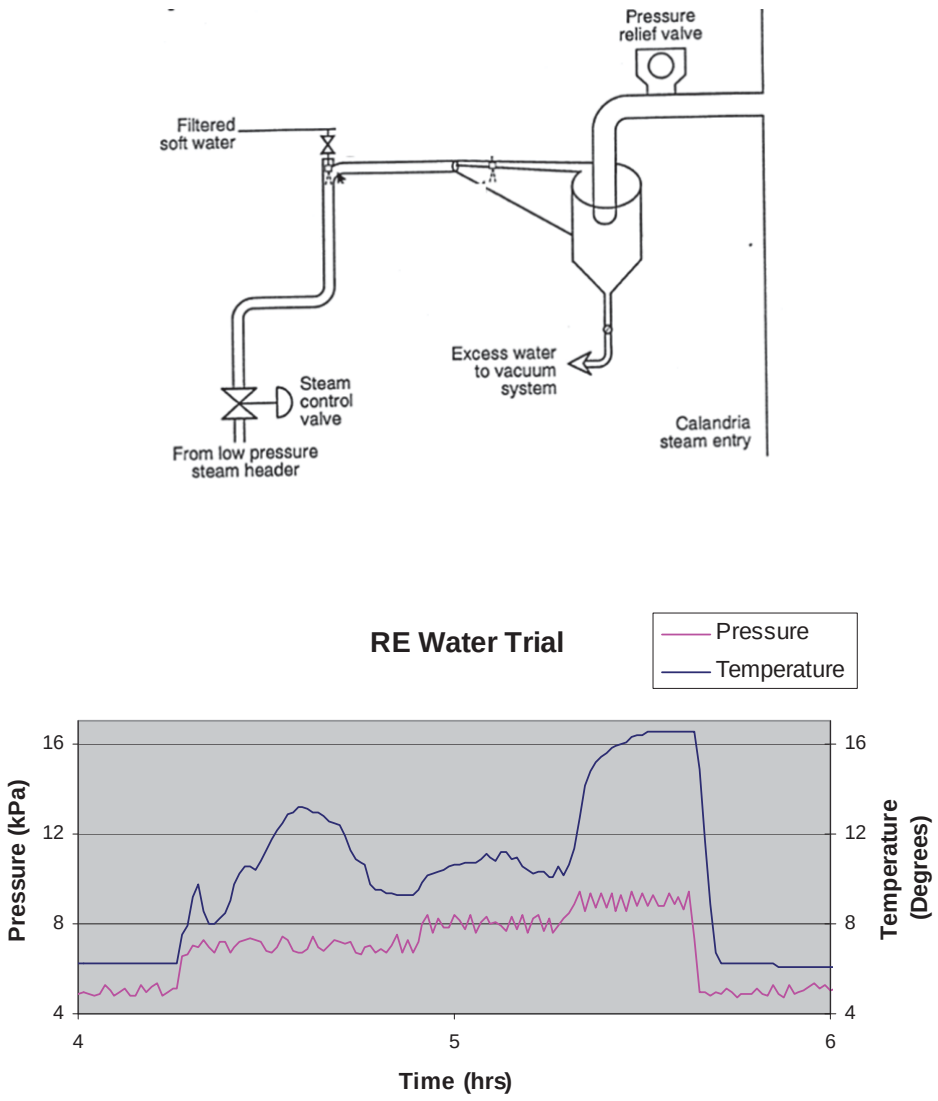

Figure 5-5: Steam differential temperature profile due to change in differential steam pressure in Effect B

The steam temperature seemed to overshoot from its saturated conditions with every step change in the steam pressure. The overshoot in the steam temperature shows that the steam was not saturated and that superheat was entering the calandria. Superheated steam makes the evaporation process very inefficient because the heat transfer coefficient for condensing saturated steam is many times more than the heat transfer coefficient for superheated steam. Hence, it was necessary to resolve this issue before the evaporator could be used for the milk trials. The data shown in Figure 5-5 is from

effect B only but similar trends were seen in effects A and C during random times in the run length. Effects D and E were relatively good in their performance with respect to de-superheating.

The de-superheat system of the RE for all effects is as shown in the Figure 5-6 below.

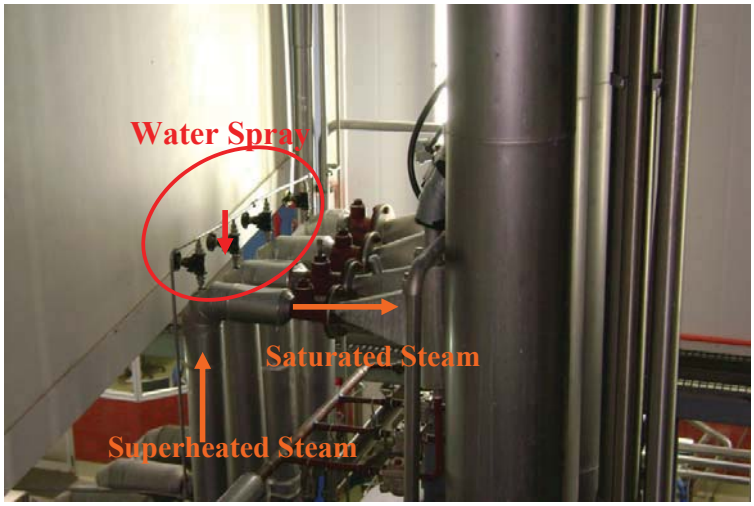

Figure 5-6: De-superheat system on Research Evaporator

Steam enters the steam control valve at 220 kPa (abs) from the low pressure steam header. Pressure is reduced to 40 kPa (abs) by the steam control valve. Water at 20 ^{o}C is sprayed into the incoming steam to fully saturate it. A small cyclone is employed to remove any excess water added during de-superheating. Excess water is flushed down through a steam trap to the condenser temperature and is extracted by the vacuum pump.

To ensure that the de-superheating system was functioning properly and all the steam entering the calandria was saturated, the amount of energy required to saturate the steam was calculated and compared to the amount of energy supplied by the water supply to de-superheat the steam. The enthalpies (kJ.kg^{-1}) were converted to equivalent volumes of water supplied and as shown in the bar chart in Figure 5-7.

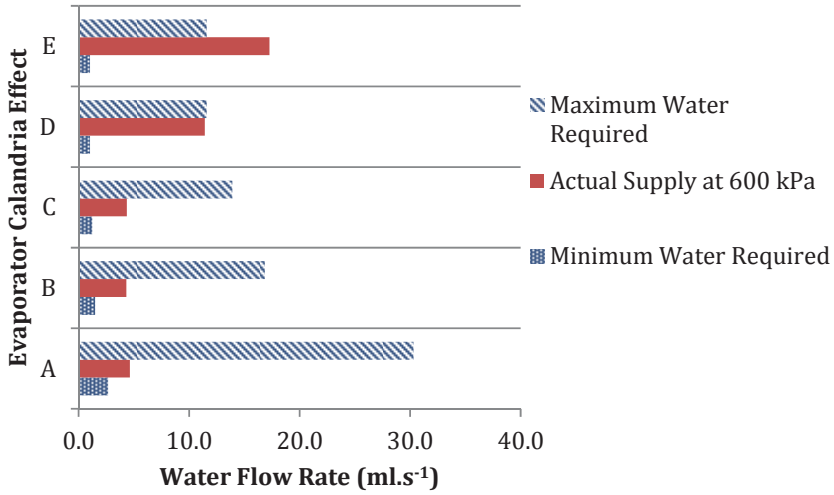

Figure 5-7: Water supply for de-superheating system

- The energy required to de-superheat the steam was calculated for the steam flow rate when the steam valve was completely open. The maximum flow rate was calculated based on the steam pressure and the steam pipe diameter.
- The minimum water requirements were calculated from the assumption that all of the water supplied at 20 ^{o}C would evaporate and that the enthalpy input to the water during sensible heating and evaporation would be used to cool down the superheated steam. On the other hand, for maximum water requirements, it was assumed none of the supplied water would evaporate and that all of the energy lost from the steam would be used for sensible heating of the water.
- The actual water flow rate from the de-superheat nozzles was measured at two different water pressures.

Abundant water was being supplied to Effects D and E but the amount of water supplied to Effects A, B and C while close to the minimum water requirement was still sufficient to de-superheat the system. When the de-superheating water line was taken down to the floor, it was realised that there was a leak in the line at effect A as shown in the Figure 5-8.

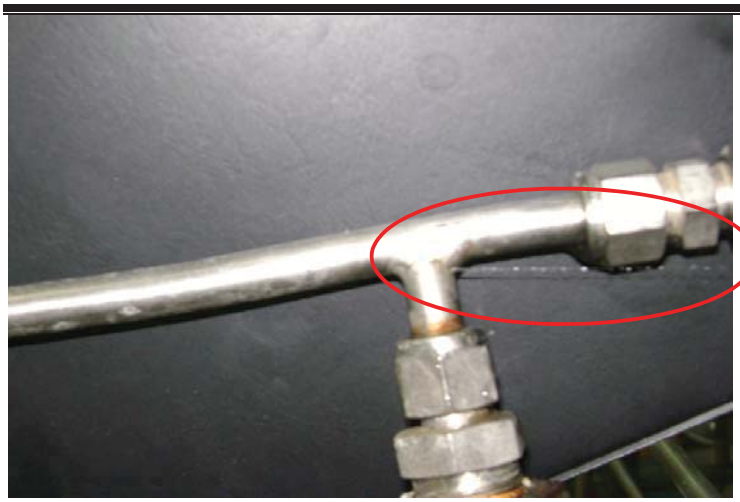

Figure 5-8: Leak in de-superheat line

All of the manual valves were rusted and many small rust elements were blocking the spray nozzles. Due to these blocks, a full cone spray pattern was not being achieved.

Figure 5-9: Rusted parts of the de-superheating line and the incomplete hollow cone spray nozzle

The plant was re-tested after the leak was fixed; the pipe cleaned and rusted parts replaced. The problem still remained unresolved.

Water flow rates were initially measured at 600 kPa (maximum pressure in the line was 650 kPa) and it was commonly seen that the water pressure would go down drastically in the pilot plant when the water from the same line was used in other equipment. Hence, higher flow rates needed to be achieved using the same water pressure to remain above the minimum water requirements. This could be done by increasing the spray nozzle diameter or replacing the hollow cone pattern spray nozzles to the full cone pattern.

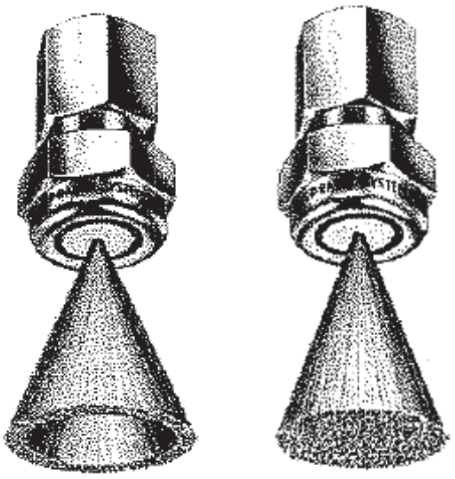

Figure 5-10: Hollow cone spray nozzle type on the left and full cone spray nozzle type on the right.

The cone pattern was changed to obtain higher water flow rates. The change finally helped in resolving the de-superheating water issue and the steam temperature obtained after testing corresponded very well with the steam pressure.

5.2.2 Trouble shooting: Non-condensable gas build up in effect C

Another problem that was regularly seen in effect C was a peculiar cyclic variation in the steam temperature and pressure (Figure 5-11).

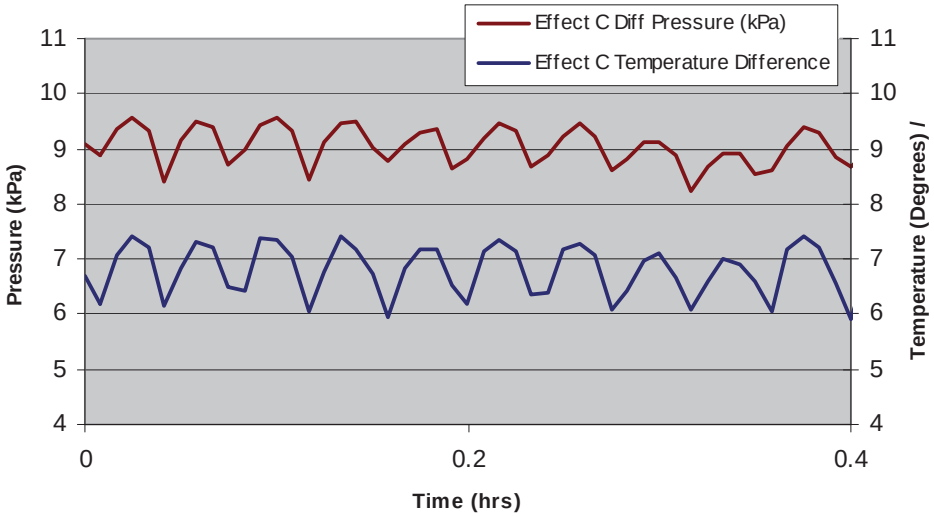

Figure 5-11: Effect C cyclic variation in steam temperature and steam pressure

A closer examination of the data revealed that the steam temperature was 2^{o}C lower than that corresponding steam saturation pressure. The pressure gauges and the temperature probes were re-calibrated to avoid any misreading. Confirming it to be a true observation, concerns were raised about the steam quality in effect C. As the same steam source was used in other effects, all of the effects were checked for such variation. It was found that this observation was unique to effect C. Further, when the milk control trial was carried out on effect B and effect C in parallel with the same set points, a lower heat transfer coefficient was found in effect C as compared with effect B at the start of the trial as shown in Figure 5-12. The reduction in the heat transfer coefficient was lower for effect C when compared to effect B.

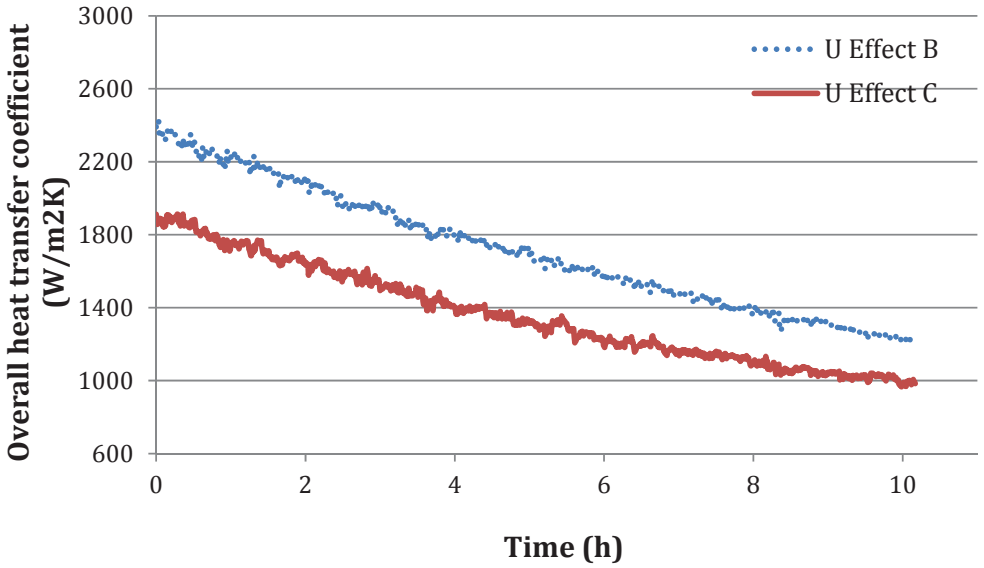

Figure 5-12: Trial RE 11. Parallel milk CONTROL trial on Effect B and Effect C

The data confirmed that the steam temperature and the temperature driving force for effect C were abnormally low given the steam pressure, which hinted at the presence of non-condensable gases in the steam.

The presence of air is known to have a marked effect on the heat transfer coefficient of the system. The presence of air is expected to be from three different sources in the calandria:

1. Quality of the incoming steam,
2. Sucking in of outside air due to a leak in the steam piping or connections,
3. Or malfunctioning of de-aeration ports that vacuum pull the NCG out of the system at the start of the run. Small quantities of steam are continuously purged out of system to make sure that NCG do not build up over time.

The option to question the quality of the incoming steam was ruled out as the same steam was supplied to other effects. All the piping and connections were checked for any vacuum leaks and old seals were replaced. The de-aeration ports were dismantled and checked to see if enough vacuum was being pulled using a manual pressure gauge. Everything seemed to be working properly except that there seemed to be a high

condensate level at the bottom of the calandria when seen from the sight glass. The Figure 5-13 shows a schematic diagram of the bottom part of the effect C calandria.

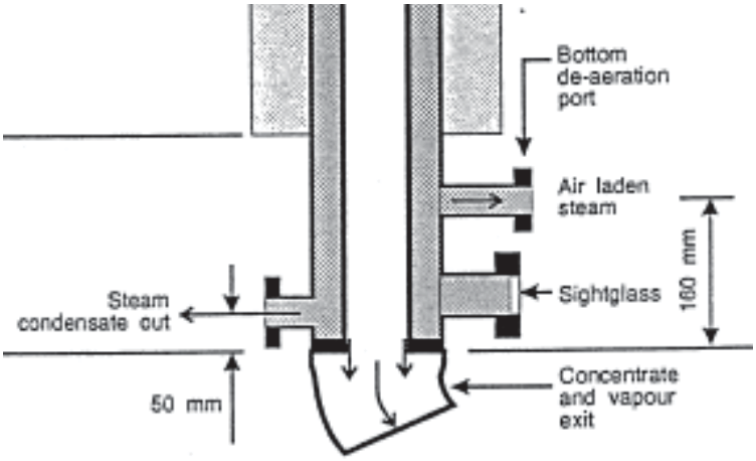

Figure 5-13: Bottom of Effect C Calandria

Condensate is driven out from the bottom of the calandria, and passes through a steam trap to the vacuum pump. The sight glass was installed for a visual check on the condensate level.

Air is heavier than steam and is known to collect at the bottom of the steam jacket. A de-aeration port was installed at the bottom for constant steam purging. At the start of each run, a vacuum was pulled on the steam side of the calandria through the de-aeration port until pressure dropped to 10 kPa (abs) before the steam valves were opened. This helped in the removal of NCG present on the steam side of the calandria.

It was clear from viewing of the sight glass that the condensate level was above the sight glass. It was not possible to know the exact level of condensate. It was thought that because the de-aeration port was just 100 mm above the sight glass level, the level of condensate would be interfering with NCG removal from the de-aeration port. Hence, it became important to fix the condensate level issue.

The condensate pipe was taken apart to check the functioning of the steam traps. Figure 5-14 shows photographs of the condensate line and the steam trap.

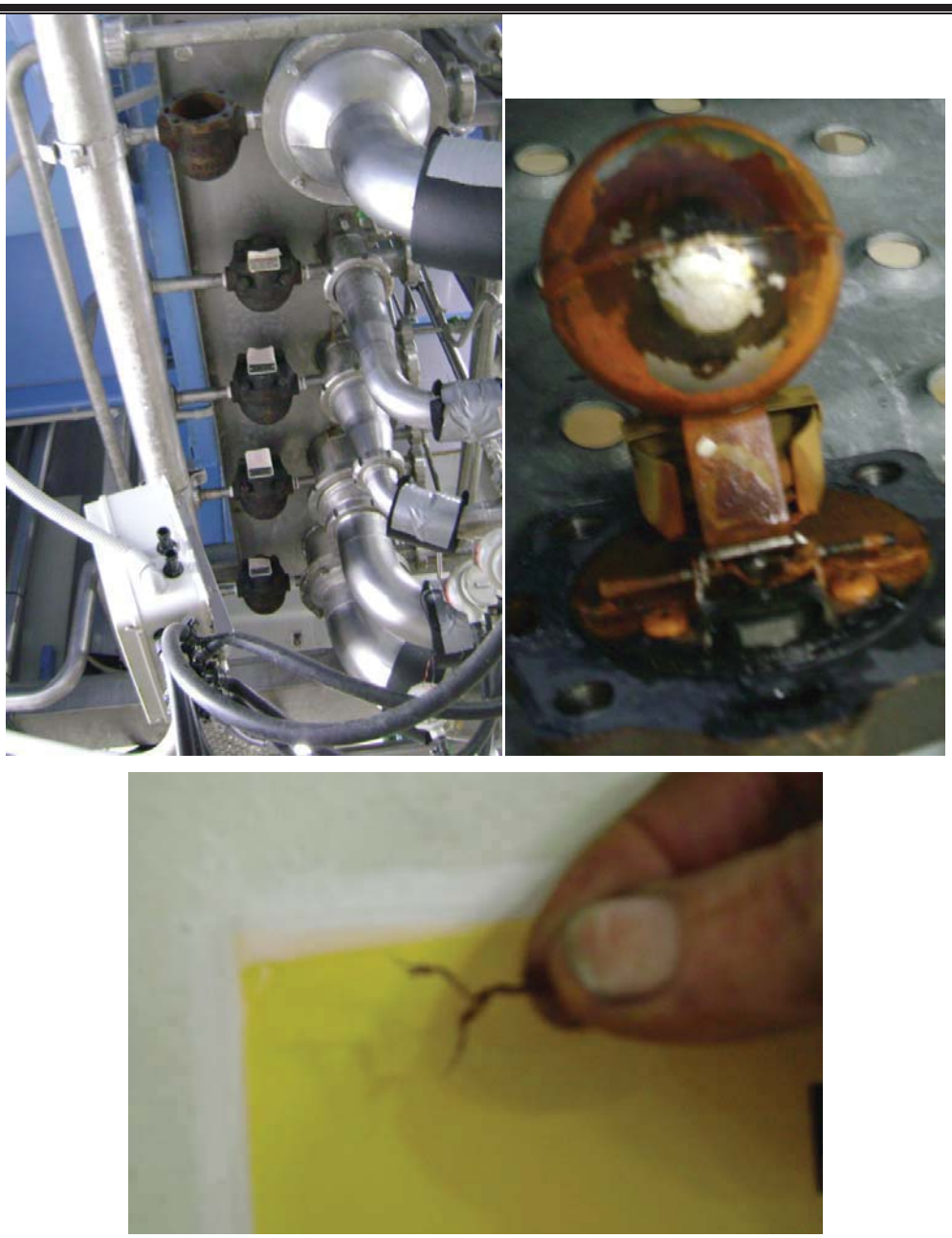

Figure 5-14: Steam trap on Research Evaporator.

Heavy rust particles were found in the steam trap. The movement of the metal float in the steam trap seemed to be getting interfered with by the rust particles. The steam traps were soaked in acid solution overnight and cleaned the following day. They were put back together in the condensate line, set up and checked for their functioning for condensate removal. The RE was started and the condensate level was checked. After cleaning, the condensate level seemed to be remaining constant at half way up the sight glass. The cyclic variation stopped. The steam temperature also correlated well with the

steam pressure, thus hinting at the fact that the condensate level was indeed the root cause leading to the NCG build-up in the effect C calandria.

5.2.3 Validation of Parallel Trials

The problem of non-condensable gases in effect C that gave rise to the cyclic variation and lack of correspondence between steam temperature and steam pressure was fixed by clearing rust particles from the steam trap. Even though this problem was fixed, the initial heat transfer coefficient in effect C at the same processing conditions was still lower than in effect B by approximately 500 $W.m^{-2}.K^{-1}$. Six milk trials (RE11-RE16) were carried out in parallel while simultaneously resolving this issue. For each trial, the same milk was processed in both effects B and C with the same processing conditions. Fouling obtained in effect C was random and there was no pattern increase or decrease of heat transfer coefficient with time. In some cases, as shown in Figure 5-15, almost no fouling was seen in Effect C.

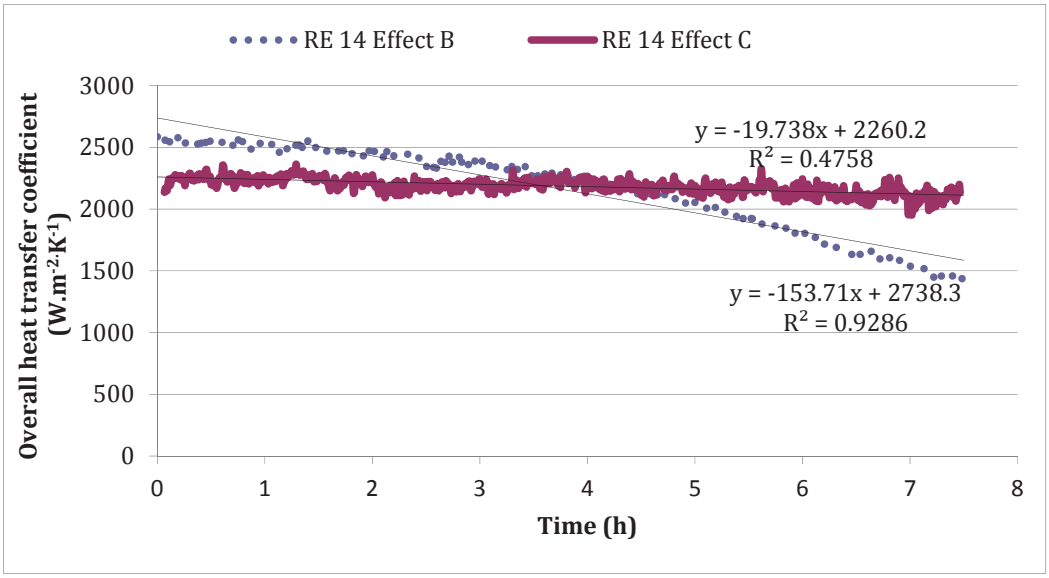

Figure 5-15: Parallel Trial: Very slight fouling in effect C

Effect C was manually opened to confirm this finding from the heat transfer coefficient plots in Figure 5-15. Figure 5-16 shows the lower ends of effects B and C. The tubes of each effect were checked. It is clear from Figures 5-17 and 5-18 that effect C showed negligible fouling deposits as compared with effect B.

Figure 5-16: Bottom of Effect B (right) and Effect C (left)

Figure 5-17: Effect B tube

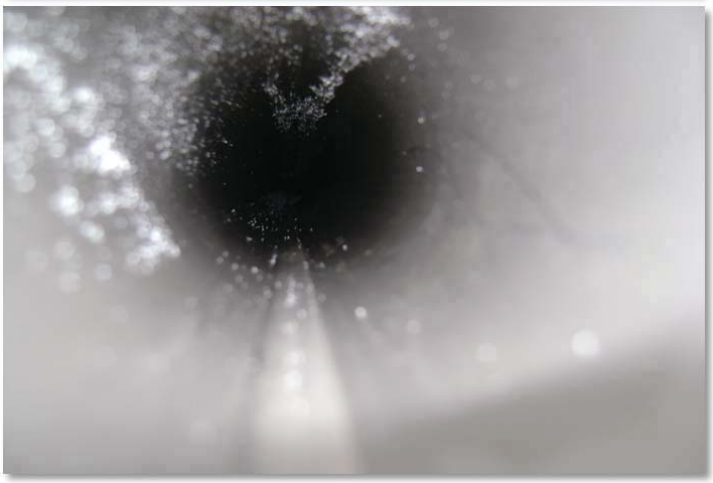

Figure 5-18: Effect C tube

It was suspected that effect C might have had a air leak, which led to lower overall heat transfer coefficient at the start of the trials and no fouling as the trial progressed. Attempts were made to resolve this issue by changing all the seals and manually checking all the fittings. Due to time constraints, this problem remained unsolved. The results of the partial investigation and the recommendation was forwarded to the maintenance department at the Fonterra Research Centre.

Due to the unresolved probable air leak issue in effect C, the parallel design trials were abandoned. Instead, series trials were carried out using just effect B, as discussed in Chapter 6.

Chapter 6

6 Series trials: Results and Discussion

Series trials were carried out using effect B after validation of the parallel trials was abandoned.

In the series trials, a control run was conducted in the morning as soon as the milk was received from milk reception in the pilot plant. Control runs usually lasted for four hours. A full CIP was carried out after the control run while the milk was stored at 4 ^{o}C. A control or coated run was carried out immediately after the CIP was finished and the processing conditions were exactly the same as in the morning run. There was an approximately six hour interval between the start of a control run and the start of a coated run. It was thought that the six hours of milk storage might have had a detrimental effect on the milk composition. Hence, control-control trials were carried out in the morning and afternoon using the same milk to account for any changes due to milk storage. The results obtained from the control-control trials were incorporated into the analysis when finding the effect of coating on fouling in the control-coating trials.

Three control-control and four control-coating runs were carried out in the series trials. The details of the all of the series trials in the morning are given in Table 6-1. The details of all the corresponding afternoon trials are given in Table 6-2. The letter ‘a’ after the trial number represents morning trials and the letter ‘b’ after the trial number represents afternoon trials. Treatment given is either control (uncoated) or coated. Product temperature is the evaporation temperature. Temperature difference is the temperature driving force (steam temperature minus product temperature). Fouling rate and induction time were calculated as mentioned in Section 4.4.

DoM	Run	TS	Rig	Trt_am	ProdTemp_am	TempDiff_am	FR_am	IT_am
22/01/10	RE 17a	13.66	B	Uncoated	79.83	4.36	239.88	0.34
26/01/10	RE 18a	13.72	B	Uncoated	79.49	4.83	234.37	1.06
28/01/10	RE 19a	14.1	B	Uncoated	79.14	4.65	221.91	0.55
29/01/10	RE 20a	13.03	B	Uncoated	79.50	4.44	161.51	0.57
1/02/10	RE 21a	14.12	B	Uncoated	79.38	4.80	270.61	0.34
2/02/10	RE 22a	13.44	B	Uncoated	79.88	4.10	217.56	0.17
3/02/10	RE 23a	14.29	B	Uncoated	79.49	4.12	250.78	0.46

Table 6-1: Morning run of the series trials

DoM	Run	TS	Rig	Trt_pm	ProdTemp_pm	TempDiff_pm	FR_pm	IT_pm
22/01/10	RE 17b	13.66	B	Coated	80.10	4.54	182.96	1.08
26/01/10	RE 18b	13.72	B	Uncoated	79.42	4.76	287.82	0.39
28/01/10	RE 19b	14.1	B	Coated	79.63	4.57	201.27	0.65
29/01/10	RE 20b	13.03	B	Uncoated	79.69	4.21	168.04	0.42
1/02/10	RE 21b	14.12	B	Coated	79.44	4.43	186.83	0.21
2/02/10	RE 22b	13.44	B	Uncoated	79.85	4.21	248.23	0.59
3/02/10	RE 23b	14.29	B	Coated	79.00	4.72	232.09	0.23

Table 6-2: Afternoon run of the series trials

KEY	
DoM	Date
TS	Total Solids
Trt	Treatment
ProdTemp	Evaporation Temperature
TempDiff	Temperature Driving Force
FR	Fouling Rate
IT	Induction Time
_am	morning run
_pm	afternoon run

6.1 Induction time and fouling rate of control-control trials

Figure 6-1 and Figure 6-2 show the induction times and the fouling rates, respectively, of the control trials. The two bars for each trial number represent the data from the morning run (1st bar) and the data from the afternoon run (2nd bar).

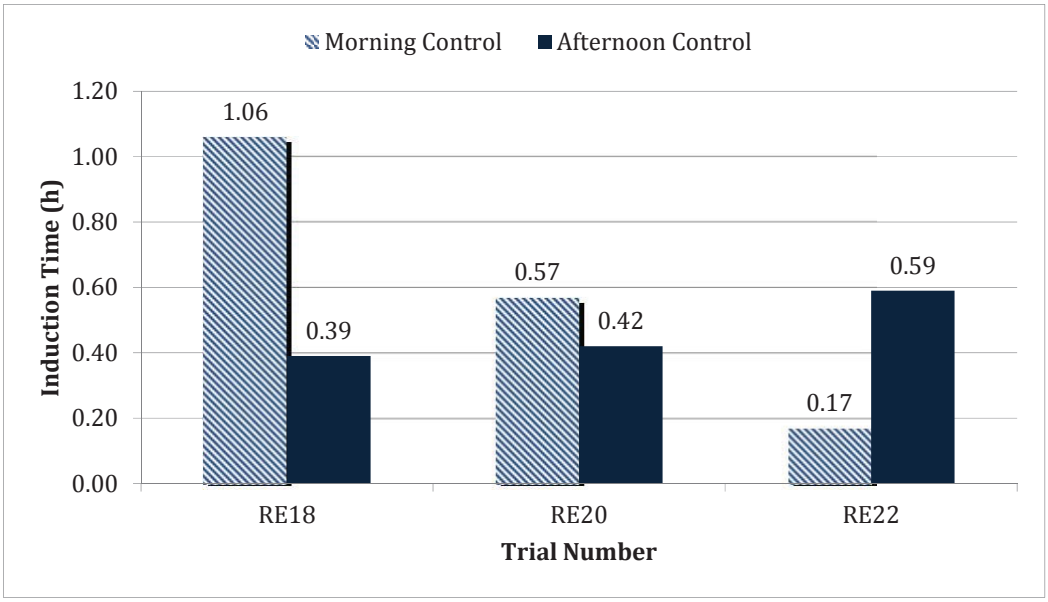

Figure 6-1: Induction times in control trials

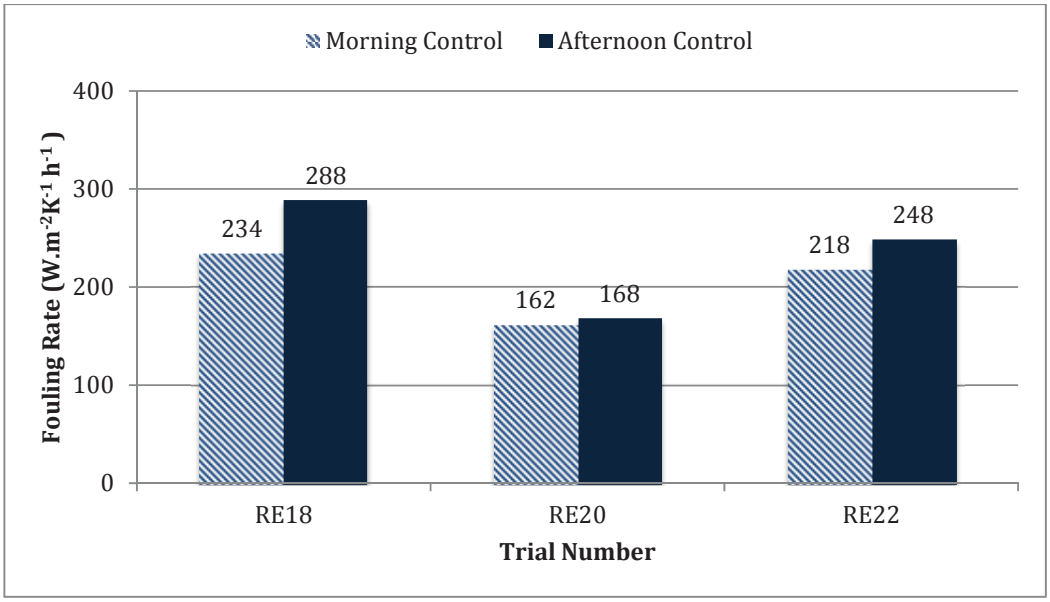

Figure 6-2: Fouling rates in control trials

Although the processing conditions were the same in all the control-control trials, the differences in induction time between morning and the afternoon runs varied with no apparent trend.

The fouling rates in the afternoon runs were consistently higher than the morning runs.

From the literature, it is known that induction time is shorter for aged milk as compared with the fresh milk (Kastanas *et al.*, 1995). Thus it was expected that the induction time in the afternoon trials would be shorter than in the morning trials. This trend was observed in trials RE 18 and RE 20 but the trend was the reverse in RE 22. The induction time is also known to be dependent on other factors such as cleanliness of the equipment, the initial interaction between the surface and individual milk components and specific changes to milk composition due to ageing (Delsing and Hiddink, 1983). Studying the interaction chemistry between the surface and the milk constituents was out of scope in this project and hence no further analysis was done to try and understand the variation in the induction time between the control runs.

The higher fouling rate in the afternoon runs was thought to be because of milk ageing or due to the unavoidable inherent differences between the runs in the evaporation temperature and temperature driving force at the start of the run or combination of these factors. The ageing effect of milk could be ignored because it was consistent for both the control-control and the control-coating trials. But it was important to investigate the inherent difference in the evaporation temperature and the temperature driving force as this difference was not consistent across all the trials.

Figure 6-3 shows differences between morning and afternoon runs in the evaporation temperature and compares it to the corresponding differences in the fouling rate, for the same milk batch. The seven data points represent seven trials (three control trials and four coating trials).

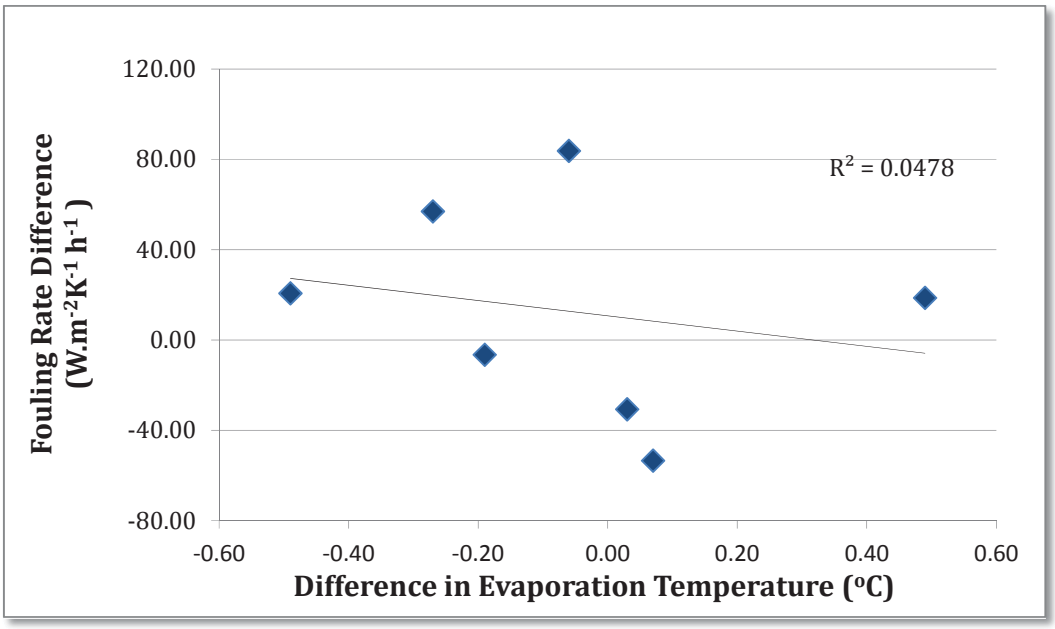

Figure 6-3: Effect of difference between morning and afternoon runs in the evaporation temperature on the corresponding difference in fouling rate.

The maximum difference in the evaporation temperature between the morning and afternoon trials was 0.49 ^{o}C.

Similarly, Figure 6-4 shows differences between the morning and the afternoon trials in the temperature driving force and compares it to the corresponding differences in the fouling rate for the same milk batch.

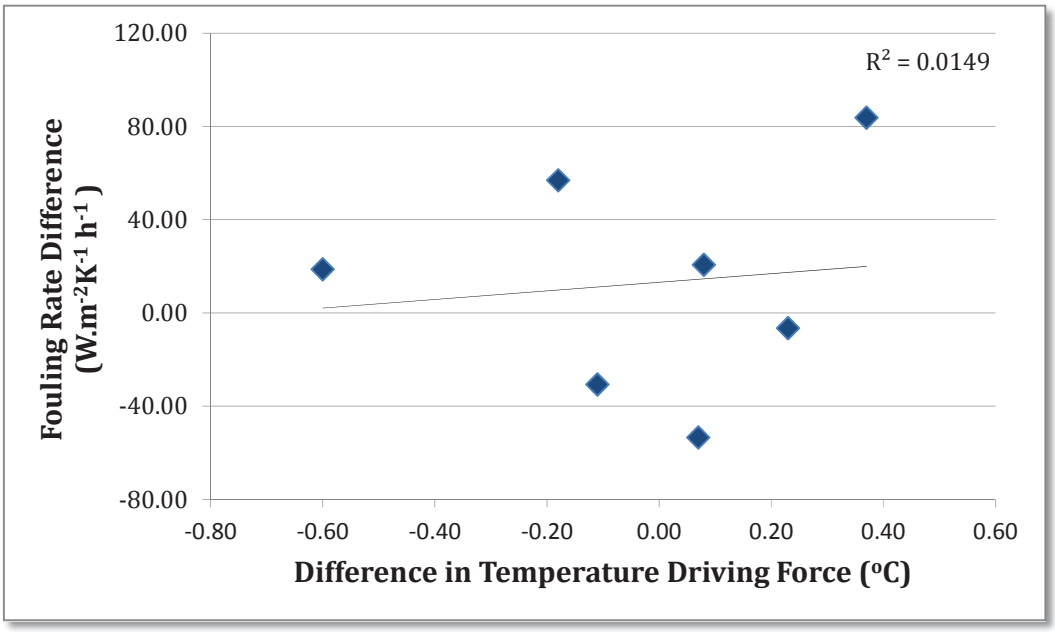

Figure 6-4: Effect of difference between morning and afternoon runs in temperature driving force on the corresponding difference in fouling rate.

The maximum difference in the temperature driving force between the morning and afternoon trials was 0.60 ^{o}C.

These differences were considered in the correlation and the regression analysis carried out while investigating the effect of coating in section 6.2.

6.2 Effect of coating on induction time and fouling rate

Figure 6-6 show the induction time and the fouling rate, respectively, of all of the series trials. Similarly to Figure 6-1, the two bars for each trial represent the morning (1st bar) and afternoon (2nd bar) runs, respectively, of the series trials. The brick pattern has been assigned to the coating runs.

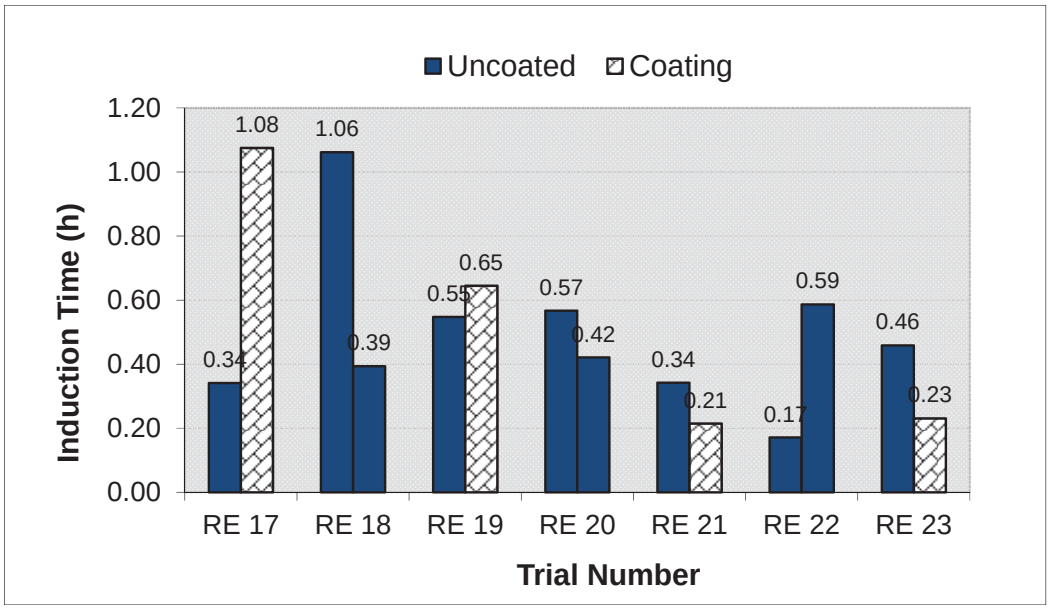

Figure 6-5: Effect of Coating on Induction times for all series trials

The induction time in the control-control runs showed a mixed trend.

The aim of the control-coating trials was to see if coating had any major impact in increasing the induction time. There was no apparent effect of coating on the induction time. The induction time was higher in RE 17 and RE 19 while it was lower in RE 21 and RE 23. As it was thought that the induction time was dependent on other unknown factors that were out of scope in this study, no further analysis was done to try and understand the effect of coating on the induction time.

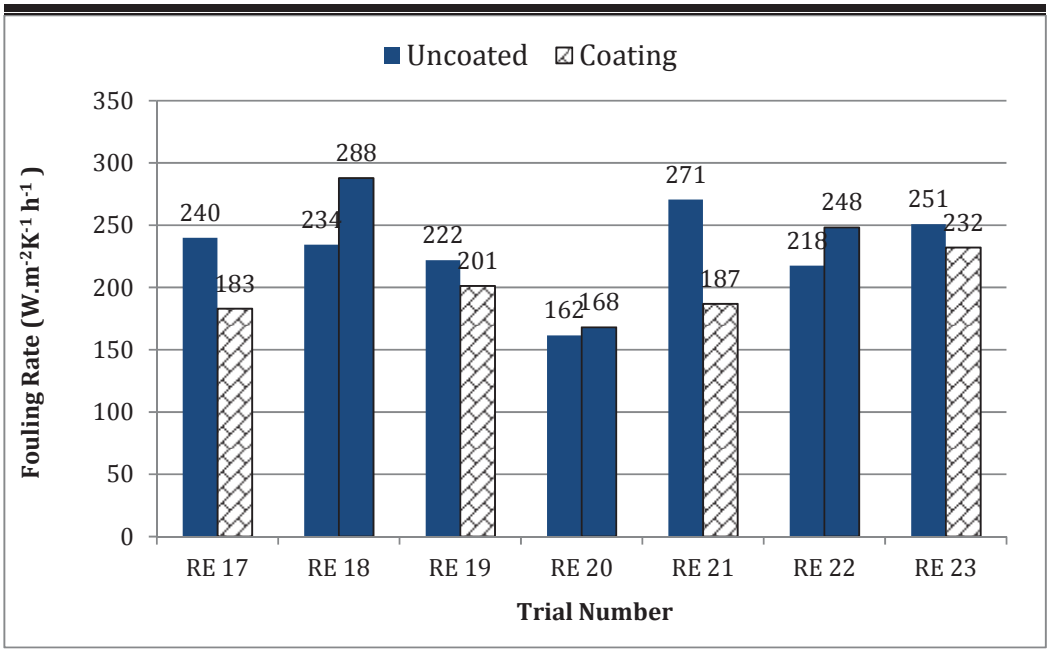

Figure 6-6: Effect of Coating on Fouling rate

In all the control-control trials, fouling rate was higher in the afternoon trials. But in all the trials where coating was applied, the trend was reversed. In all the afternoon coating trials fouling was less than the morning control trials.

A Pearson's correlation coefficient test was carried out on each factor that was different in afternoon run as compared to the morning run using the seven data points.

	Difference in Coating/No Coating	*Difference in Temperature Driving Force*	*Difference in Product Temperature*	*Fouling Rate Difference*
Difference in Treatment	1			
Difference in Temperature Driving Force	-0.246	1		
Difference in Evaporation Temperature	-0.091	-0.608	1	
Difference in Fouling Rate	0.840	0.122	-0.219	1

Table 6-3: Results of Pearson's correlation coefficient test on difference between morning and afternoon runs

Difference between morning and afternoon runs in the evaporation temperature, temperature driving force and treatment (coating/no coating) were correlated to the

corresponding differences in fouling. A correlation coefficient of 0.84 in the fourth row shows that there was a strong dependence of difference in fouling rate on difference in treatment. The dependence of difference in fouling rate on difference in temperature driving force and on difference in evaporation temperature was weak.

A regression test was carried out using all three factors (differences in treatment, temperature driving force and evaporation temperature) with difference in fouling rate as the dependent variable (Table 6-4).

	p-value
Diff in Treatment (Coating)	0.033
Diff in Temp Driving Force	0.263
Diff in Evaporation Temperature	0.691

Table 6-4: Regression test of difference in fouling rate

It revealed that for treatment (coating) the p-value was 0.033. This means that, at the 96.7% level of confidence, the difference in fouling rate between morning (uncoated) and afternoon (coated) runs was due to the coating in the afternoon runs. As the fouling rate was always lower in the afternoon runs, it can be concluded, at the above level of confidence, that the coating had a beneficial effect in terms of reducing fouling rate.

The dependence of fouling rate difference on difference in evaporation temperature and difference in temperature driving force was very low (Table 6-4).

6.3 Discussion

Fundamental studies carried out by other researchers have shown that silicate based transient coating helps in conditioning the surface and inhibits the initial interaction between the minerals in the milk and the oxide layer on the stainless steel surface layer (Parbhu *et al.*, 2006). It is considered that once the initial interactions are complete the fouling phenomenon shifts from surface-foulant interaction to foulant-foulant interaction. After the fouling phenomenon shifts to foulant-foulant interaction, the coating has no effect in reducing further deposit build-up.

If this hypothesis is considered true, it would be expected that the coating would increase the induction time and consequently delay the fouling process. In the results obtained from this work, the induction time data for the control trials displayed random variation due to unknown factors, and the effect of coating on the induction time could not be clearly stated. It thus remains unclear whether the coating indeed had an effect on induction time, as no significant effect has been shown in these trials.

The fouling rate was consistently lower in the coating trials compared with the control trials. This suggests that even though the induction time data did not prove the effect of coating, the overall fouling data showed that coating resulted in a reduction in deposit build-up.

The results presented by other researchers (Parbhu *et al.*, 2006) were based on experiments done under conditions of convective heat transfer. No study has been found that reports the effect of transient coating under the boiling heat transfer conditions.

It is thought that the effect of coating in reducing fouling under boiling heat transfer conditions could be due to the following reason:

- *Improving the liquid coverage* of the falling film on the surface due the coating's hydrophilic nature. As the coverage is increased fewer hot-spots would be created, thus reducing fouling caused due to burn-on of milk solids at these hot-spots.

In-depth study to investigate these factors individually was out of scope in this work, and hence it is recommended that fundamental work to be carried out to help understand the actual principle underlying the effect of coating in reducing overall fouling. These conclusions are based on only 7 trials and therefore this work should be replicated to confirm the findings.

6.4 Estimation of increase in run time due to coating

Coating has shown to be statistical significant in reducing the fouling rate. All the coating trials showed a reduction in fouling rate when compared with the control trials. The amount of reduction in the fouling rate varied from trial to trial. The factors affecting the variation in the fouling reduction due to coating was not studied in this project.

The aim of conducting the coating trials was to see the effect of coating on reducing fouling and eventually estimate the increase in the run length. The increase in the run length calculations shown below are based on the following assumptions:

- The average of the differences in fouling rate between three control-control morning and afternoon runs MINUS the average of the differences in fouling rate between four control-coated morning and afternoon runs were taken to estimate the increase in the run length due to coating
- The average differences in the fouling rate between the control-control and control-coating trials were for the duration of four hours of total run time.
- All the coating trials were carried out on milk aged for 6 hours as compared to the corresponding control trials.
- All the trials were conducted on the falling film evaporator in the pilot plant of Fonterra Research Centre.

The calculations are as follows.

$$\%\ \text{increase in run length} = \frac{(\text{Average diff in FR})_{\text{control trials}} - (\text{Average diff in FR})_{\text{coating trials}}}{\text{Average of FR of all series trials}} * 100$$

$$\% \text{ increase in run length}$$

$$= \frac{(-30.22\ [\mathrm{W}.m^{-2}K^{-1}h^{-1}]) - (45.01[\mathrm{W}.m^{-2}K^{-1}h^{-1}])}{221.70\ [\mathrm{W}.m^{-2}K^{-1}h^{-1}]} * 100$$

$$\% \ increase\ in\ run\ length = 34\ \%$$

The basic calculations show that the coating has a potential to increase the run length by 33.92%. This can be considered as just a preliminary indication of the potential of coating in increasing the run length. For more robust estimation, more trials should be carried out with longer experimental run times.

Chapter 7

7 Conclusion

Fouling of heat processing equipment is a major problem in the dairy industry and creates the need for frequent cleaning thus restricting the production run length. Benefits can be obtained by reducing fouling and increasing the production run length and hence there is a drive in Fonterra to investigate fouling mitigation techniques.

This project investigated a coating which is temporary in nature and can be used on a regular basis. Very little capital cost is needed to employ this technology in an existing production line in the factory and thus reduction in fouling due to transient coating technology was an important topic for investigation. Preliminary laboratory scale work at Fonterra reported a silica based coating was successful in reducing fouling under convective heat transfer conditions. This project was set up to test the efficacy of coating under the nucleate boiling heat transfer conditions found in falling film evaporators, on a pilot scale.

A literature review on fouling established that fouling was the result of a complex interaction between milk properties such as total solids, composition and pH, surface properties such as surface charge, wettability and roughness, and processing conditions such as the heat transfer mechanism, temperature, flow conditions and equipment geometry. The learning from the literature review helped in recognizing the factors that could affect fouling in this work and thus, in the experimental design, all the recognised factors were controlled.

Parallel design was implemented that used two identical effects of the RE for carrying out control and coated trials at the same time using the same milk. The validation experiments showed that one of the effects had a vacuum leak which could not be resolved, and hence the parallel trials were abandoned. The approach was changed to that of conducting trials in series on just one effect. The uncontrolled effect of ageing was accounted for by carrying out control runs in series (control-control) using the same

milk and comparing the results with those obtained from equivalent control-coating runs.

Three control-control runs and four control-coating runs were carried out to investigate the change in fouling rate due to coating. Fouling rate of the afternoon runs was consistently higher in the control-control trials suggesting the possible effect of ageing on fouling. The induction time varied randomly within the control-control trials suggesting the effect of other unknown factors that was not further analysed. Because the variation of induction time in the control-control trials was random, the change in induction time due to the effect of coating could not be determined. All the coating trials showed consistently lower fouling rate as compared with their corresponding control trials. The Pearson's correlation coefficient of 0.83 showed a strong effect of coating on the fouling rate. Further, a regression analysis gave a P value of 0.033, representing a significant effect of coating on the fouling rate at the 96.7% level of confidence. The extent of reduction in fouling rate varied from trial to trial.

From the basic calculations using the averages of the fouling rate morning-afternoon differences in the control-control trials and in the control-coating trials, it was estimated that the coating had a potential to increase the run length by 34 % under the conditions existing in these experiments. It is suggested that more trials should be carried out to gain a more robust quantitative estimation of the increase in run length.

Work beyond the scope of the data presented here will be required further to investigate the differences in the fouling rate found between the morning control and afternoon control runs, the variation in the induction time between the morning control and afternoon control runs, the effect of coating on the change in induction time, specific factors of coating that help in reducing the overall fouling rate and the factors that caused a higher decrease in fouling rate in some coating trials compared with other coating trials.

Chapter 8

8 References

Anema, S., Lowe, E. K. and Li, Y. (2003). "Effect of pH on the viscosity of heated reconstituted skim milk." International Dairy Journal 14(6): 541-48.

Bansal, B. and Chen, X. D. (2006). "A critical review of milk fouling in heat exchangers." Comprehensive Reviews in Food Science and Food Safety 5(2): 27-33.

Belmar-Beiny, M. T. and Fryer, P. J. (1993). "Preliminary stages of fouling from whey-protein solutions." Journal of Dairy Research 60(4): 467-83.

Billet, R. (1989). "Evaporation Technology - Principles, Applications, Economics." VCH Verlagsgescllschaft mbH, Weinheim, Germany.

Bouman, S., Waalewijn, R., De Jong, P. and Van Der Linden, H. J. L. J. (1993). "Design of falling-film evaporators in the dairy industry." Journal of the Society of Dairy Technology 46(3): 100-06.

Britten, M., Green, M. L., Boulet, M. and Paquin, P. (1988). "Deposit formation on heated surfaces - effect of interface energetics." Journal of Dairy Research 55(4): 551-62.

Burton, H. (1965). "A method for studying factors in milk which influence deposition of milk solids on heated surface." Journal of Dairy Research 32(1): 65-&.

Burton, H. (1968). "Reviews of the progress of dairy science: Section G. Deposit from the whole milk heat treatment plant - a review and discussion." Journal of Dairy Research 35: 317-30.

Chen, H. (1997). Heat Transfer and Fouling in Film Evaporators with Rotating Surfaces. Department of Food Technology. Palmerston North, Massey University. PhD.

Chen, H. and Jebson, R. S. (1997). "Factors Affecting Heat Transfer in Falling Film Evaporators." Food and Bioproducts Processing 75: 111-16.

Chen, P. (2002). "An apparatus designed for falling film boiling behaviour investigation " Fonterra Research Centre, Palmerston North

Daufin, G., Labbe, J. P., Quemerais, A., Brule, G., Michel, F., Roignant, M. and Priol, M. (1987). "Fouling of a heat-exchange surface by whey, milk and model fluids - an analytical study." Lait 67(3): 339-64.

de Jong, P. (1997). "Impact and control of fouling in milk processing." Trends in Food Science & Technology 8(12): 401-05.

Delsing, B. M. A. and Hiddink, J. (1983). "Fouling of heat transfer surfaces by dairy liquids." Netherlands Milk and Dairy Journal 37(3): 139-48.

Duker, B. (2010). Personal Communication. Fonterra Research Centre, Palmerston North.

Foster, C. L., Britten, M. and Green, M. L. (1989). "A model heat exchange apparatus for the investigation of fouling of stainless steel surfaces by milk. 1. Deposit formation at 100 ^{o}C." Journal of Dairy Research 56(2): 201-09.

Fryer, P. J., Christian, G. K. and Liu, W. (2006). "How hygiene happens: physics and chemistry of cleaning." International Journal of Dairy Technology 59(2): 76-84.

Fung, L., McCarthy, O. and Tuoc, T. (1998). "The effect of fat globule membrane damage on fouling of whole milk." Fouling and cleaning in food processing'98. Cambridge, U.K.

Galani, D. and Apenten, R. K. O. (1999). "Heat-Induced Denaturation and Aggregation of ß-Lactoglobulin: Kinetics of Formation of Hydrophobic and Disulphide-Linked Aggregates." International Journal of Food Science and Technology 34: 467-76.

Hadfield, J. (2007). "Mitigating Fouling with Transient Coating." Fonterra Co-operaitve Group Ltd.

Housova, J. (1970). "Heat transfer in falling-film evaporators." Prumysl Potravin 21(1 Suppl).

Incropera, F. P. and DeWitt, D. P. (1990). "Fundamentals of Heat and Mass Transfer." John Wiley & Sons, New York 3rd edn.

Jeurnink, T., Verheul, M., Stuart, M. C. and deKruif, C. G. (1996a). "Deposition of heated whey proteins on a chromium oxide surface." Colloids and Surfaces B-Biointerfaces 6(4-5): 291-307.

Jeurnink, T. J. M. and Brinkman, D. W. (1994). "The cleaning of heat exchangers and evaporators after processing milk or whey." International Dairy Journal 4(4): 347-68.

Jeurnink, T. J. M. and Dekruif, K. G. (1995). "Calcium-concentration in milk relation to heat stability and fouling." Netherlands Milk and Dairy Journal 49(2-3): 151-65.

Jeurnink, T. J. M., Walstra, P. and deKruif, C. G. (1996). "Mechanisms of fouling in dairy processing." Netherlands Milk and Dairy Journal 50(3): 407-26.

Kang, C. and Lee, Y. (2007). "The surface modification of stainless steel and the correlation between the surface properties and protein adsorption." Journal of Material Science(18): 1389-98.

Karlsson, C. A.-C. (1999). Fouling and Cleaning of Solid Surfaces: The Influence of Surface Characteristics and Operating Conditions. Food Engineering, Lund University. PhD.

Kastanas, P., Ravanis, S., Lewis, M. J. and Grandison, A. S. (1995). "Effects of raw-milk quality on fouling at UHT conditions." Journal of the Society of Dairy Technology 48(3): 97-99.

Krisdhasima, V., McGuire, J. and Sproull, R. (1992). "Surface hydrophobic influences on beta-lactoglobulin adsorption kinetics." Journal of Colloid and Interface Science 154(2): 337-50.

Mackereth, A. R. (1995). "Thermal and Hydraulic Aspects of Falling Film Evaporation." The University of Canterbury, Christchurch, New Zealand PhD.

Mackereth, A. R. and Grant, J. E. (1998). "Comparative Evaporator Fouling Losses for Whole Milk and Skim Milk." New Zealand Dairy Research Institute.

Masse, (2007). "The Market for Whey Products", Fonterra Co-operative Group, Palmerston North, New Zealand.

Müller-Steinhagen, H. and Branch, C. A. (1997a). "Heat transfer and heat transfer fouling in Kraft Black Liquor Evaporators." Experimental Thermal and Fluid Science(14): 425-37.

Müller-Steinhagen, H. and Branch, C. A. (1997b). Heat Transfer and Heat Transfer Fouling in Kraft Black Liquor Evaporators. New York, NY, Etats-Unis, Elsevier.

Norde, W. and Haynes, C. A. (1994). Reversibility and the mechanism of protein adsorption. Symposium on Proteins at Interfaces II - Fundamentals and Applications, at the 207th National Meeting of the American-Chemical-Society, San Diego, Ca.

Parbhu, A., Hendy, S. and Danne, M. (2006). "Reducing Milk Protein Adhesion Rates: A Transient Surface Treatment of Stainless Steel." Food and Bioproducts Processing 84(4): 274-78.

Parbhu, A. N., Soltis, J., Chen, L. Q., Atkin, J. and Hendy, S. (2004). "Specific ion binding influences on surface potential of chromium oxide." Current Applied Physics 4(2-4): 152-55.

Parris, N. and Baginski, M. A. (1991). "A Rapid Method for the Determination of Whey Protein Denaturation." Journal of Dairy Science 74(1): 58-64.

Patil, G. R. and Reuter, H. (1986). "Deposit formation in UHT plants. I. Effect of forewarming in indirectly heated plants." Milchwissenschaft-Milk Science International 41(6): 337-39.

Rebmann, H. (2008). "Use of surface coatings to mitigate dairy fouling." Fonterra Co-operative Group Ltd

Rebmann, H. (2007). "Mitigation of Dairy Fouling using Transient Coatings" Fonterra Co-operative Group Ltd.

Rosmaninho, R., Rocha, F., Rizzo, G., Müller-Steinhagen, H. and Melo, L. F. (2007). "Calcium phosphate fouling on TiN-coated stainless steel surfaces: Role of ions and particles." Chemical Engineering Science 62(14): 3821-31.

Rosmaninho, R., Santos, O., Nylander, T., Paulsson, M., Beuf, M., Benezech, T., Yiantsios, S., Andritsos, N., Karabelas, A., Rizzo, G., Müller-Steinhagen, H. and Melo, L. F. (2007b). "Modified stainless steel surfaces targeted to reduce fouling - Evaluation of fouling by milk components." Journal of Food Engineering 80(4): 1176-87.

Rosmaninho, R., Visser, H. and Melo, L. (2001). Influence of the surface tension components of stainless steel on fouling caused by calcium phosphate, Coimbra, Portugal.

Santos, O., Nylander, T., Rosmaninho, R., Rizzo, G., Yiantsios, S., Andritsos, N., Karabelas, A., Müller-Steinhagen, H., Melo, L., Boulangé-Petermann, L., Gabet, C., Braem, A., Trägårdh, C. and Paulsson, M. (2004). "Modified stainless steel surfaces targeted to reduce fouling--surface characterization." Journal of Food Engineering 64(1): 63-79.

Santos, O., Nylander, T., Schillén, K., Paulsson, M. and Trägårdh, C. (2006). "Effect of surface and bulk solution properties on the adsorption of whey protein onto steel surfaces at high temperature." Journal of Food Engineering 73(2): 174-89.

Singh, H. and Creamer, L. K. (1991). "Changes in size and composition of protein aggregates on heating reconstituted concentrated skim milk at 120-degrees-C." Journal of Food Science 56(3): 671-77.

Srichantra, A. (2008). Studies of UHT-plant fouling by fresh, recombined and reconstituted whole milk: Effect of preheat treatments. Institution of Food Nutrition and Human Health. Palmerston North, Massey University. PhD.

Tissier, J. P., Galeotti, M. A. and Lalande, M. (1985). "Experimental and analytical study of milk deposit formation on heated stainless steel surfaces." Fouling and cleaning in food processing. Second International Conference, Madison, Wisconsin, July 14-17, 1985: 178-202.

Visser, J. and Jeurnink, T. J. M. (1997). "Fouling of Heat Exchangers in the Dairy Industry." Experimental Thermal and Fluid Science 14: 407-24.

Wahlgren, M. and Arnebrant, T. (1990). "Adsorption of beta-lactoglobulin onto silica, methylated silica and polysulfone." Journal of Colloid and Interface Science 136(1): 259-65.

Walstra, P. and Jenness, R. (1984). Dairy Chemistry and Physics, Canada: John Wiley & Sons, Inc.

Wood, P A (1982) Physical Properties of Dairy Products. Technical Report T2/82. Hamilton, New Zealand: Ministry of Agriculture and Fisheries

Ye, A., Singh, H., James Oldfield, D. and Anema, S. (2004). "Kinetics of heat-induced association of ß-lactoglobulin and α-lactalbumin with milk fat globule membrane in whole milk." International Dairy Journal 14(5): 389-98.

Ye, A., Singh, H., Taylor, M. and Anema, S. (2005). "Disruption of fat globules during concentration of whole milk in a pilot scale multiple-effect evaporator." International Journal of Dairy Technology 58(3): 143-49.

Yoon, Y. and Lund, D. B. (1994). "Magnetic treatment of milk and surface-treatment of plate heat exchangers effect on milk fouling." Journal of Food Science 59(5): 964-69.

Chapter 9

9 Appendix

9.1 Appendix A

h_f

Enthalpy of Milk at specific temperature and total solids (calculated according to Cheng's paper - *OPERABILITY AND FLEXIBILITY OF A MILK PRODUCTION LINE)*

Milk Enthalpy

A new milk enthalpy correlation has been developed for the milk production process simulation according to the experimental measurements of Riedel (1976) in order to keep consistent with PRO/II system. The correlation is given as follows.

$$H = x_w H_w + x_n H_n + x_f H_f + (1 - x_f) C_f \qquad (A-10)$$

$$H_w = 5.5556 \times 10^{-5} \left(\sum_{i=1}^{6} C_i T^{(i-1)} + C_7 \ln(C_8 - T) + 4.5576 \times 10^6 \right) \qquad (A-11)$$

$$H_f = 114.2950 + 5.1381T - 3.7272 \times 10^{-2} T^2 + 1.2686 \times 10^{-4} T^3 \qquad (A-12)$$

$$H_n = 261.50 + 2.5143T - 9.7986 \times 10^{-3} T^2 + 8.2721 \times 10^{-5} T^3 \qquad (A-13)$$

$$C_f = 155.0154 \qquad (A-14)$$

where H is the enthalpy of milk (kJ kg^{-1}); H_w and H_f are the enthalpy of pure liquid water and pure fat (kJ kg^{-1}), respectively; H_n is the enthalpy of the rest component; T is the system temperature (°C); x_w and x_f are the water and fat composition (weight fraction), respectively. Equation (A-11) is taken from PRO/II for the water enthalpy calculation. In equation (A-10), the x_n is calculated as

$$x_n = 1 - x_w - x_f \qquad (A-15)$$

In equation (A-15), the x_w and x_f are the water and fat composition in weight fraction. In the correlation, the term C_f is a correction to non-ideal mixing in the milk solution. The equation is valid for temperature range 0–80°C and fat content range 0.01–100% (wt). The coefficients of equation (A-11) are given in Table A1. The average prediction error is less than 5% comparing with the experimental data of Riedel (1976).

Table A1. Coefficients of water enthalpy equation (A-11).

Coefficient	Value	Coefficient	Value
C_1	1.1875×10^7	C_2	70312
C_3	−14.616	C_4	5.0587×10^{-2}
C_5	-3.5611×10^{-5}	C_6	1.0694×10^{-7}
C_7	-1.9961×10^6	C_8	380.0